The Pennsylvania State University
The Graduate School

COLLECTIVE INVASION IN HETEROGENEOUS BLADDER CANCER TUMORS

A BIOMANUFACTURING APPROACH

A Dissertation in
Mechanical Engineering
by
Peter C. Torab

Submitted in Partial Fulfillment
of the Requirements
for the Degree of

Doctor of Philosophy

December 2020

The dissertation of Peter C. Torab has been reviewed and approved by the following:

Pak Kin Wong
Professor of Mechanical Engineering and Biomedical Engineering
Dissertation Advisor
Chair of Committee

William O. Hancock
Professor of Biomedical Engineering
Chair of the Intercollege Graduate Program in Bioengineering

Jing Du
Assistant Professor of Mechanical Engineering

Tak Sing Wong
Associate Professor of Mechanical Engineering

Daniel Haworth
Professor of Mechanical Engineering
Associate Head for Graduate Programs

ABSTRACT

Bladder cancer is an increasingly common malignancy, and muscle invasive bladder cancer is associated with particularly high rates of morbidity and mortality. The morphologic and molecular diversity of bladder cancer poses significant challenges in elucidating the invasion mechanisms responsible for disease progression. Furthermore, conventional invasion assays do not provide a physiological context for studying bladder cancer invasion within 3D microenvironments and have limited ability to capture the contribution of cellular phenotypic and molecular heterogeneity to disease progression. Here, we describe the development of biomanufactured three-dimensional (3D) microtumor invasion models suitable for the analysis of collective invasion in cancer cell lines and primary tumor cells while accounting for the heterogeneity of bladder cancer. These models incorporate a self-assembly approach for recapitulating features of bladder cancer tumors in 3D microenvironments and probing the invasive cell subpopulations. The gene expression profiles of invading microtumors were analyzed by incorporating gold-nanorod-locked-nucleic-acid (GNR-LNA) biosensors. Incorporation of single cell biosensors and transient gene knockdown into the system revealed the formation of invasive leader cells with upregulated Delta-like ligand 4 (DLL4) expression, as well as the role of NOTCH1-DLL4 signaling in collective bladder cancer invasion. The involvement of DLL4 expressing cells in bladder cancer invasion was also observed in patient samples obtained from transurethral resection. Collectively, this study demonstrates a biomanufactured 3D invasion assay approach for investigating collective invasion in bladder cancer microtumors with cellular and molecular heterogeneity, including those generated from patient-derived samples, toward personalized medicine applications.

Table of Contents

List of Tables

List of Figures

Acknowledgements

I would first like to thank my advisor, Professor Pak Kin Wong, for inspiring our research topics and creating an environment that encourages learning, creativity, and personal growth within our lab. I would also like to thank my committee members: Professor William Hancock, Professor Jing Du, and Professor Tak Sing Wong, for their guidance and insights.

I am grateful to have collaborated with experts including: Dr. David Degraff and Dr. Hironobu Yamashita of Penn State Milton S. Hershey Medical Center, and Dr. Chris Puleo and Dr. Christine Surrette of GE Global Research.

I would like to thank my current lab members, including Samuel Vilchez, Eric Ninghao Zhu, Lilly Yue Yan, Gary Jyong-Huei Lee, Sara Korsunsky, and Britney Forsyth, and lab alumni, including Dr. Yi Lu, Dr. Jian Gao, Dr. Yuan Xiao, Dr. Ying Wan, Dr. Shue Wang, Dr. Hui Li, and Tyler Malcom for contributing to a stimulating work environment.

I would like to thank my parents, Jennifer Stockton and Hamid Torab, and my brother, Philip Torab, who sparked my interest in science and engineering and supported me throughout my education and training. I would also like to thank Haley Sabitus for always supporting me and believing in me.

Chapter 1

Introduction

1.1 Bladder Cancer Overview

Bladder cancer is the second most common genitourinary malignancy in the United States and is associated with high treatment costs and poor patient outcomes. Early stage or non-muscle invasive bladder cancer (NMIBC) accounts for 75% of new cases, is often recurrent (50-70% recurrence rate),[1] and manifests occasionally with progression to locally advanced or muscle invasive disease (10-15% progression rate).[1–4] In contrast, advanced muscle invasive bladder cancer (MIBC), which accounts for 25% of new cases, is especially lethal, with a five-year survival rate of less than 50%.[1,3] In addition, 50% of muscle invasive bladder cancer patients experience disease recurrence, usually in the form of metastatic disease which is almost uniformly lethal.[1]

Several recent studies have highlighted the importance of personalized treatment strategies in improving patient outcomes.[2,4] Unfortunately, such strategies are hampered by inaccurate prognostication, inconsistency in management programs, and varying patient response to therapies.[2] It is widely believed that the cellular and molecular heterogeneity associated with bladder cancer tumors contributes to these differences in progression, recurrence, and treatment response. However, the role of intratumoral heterogeneity in progression and the mechanisms of tumor invasion remain poorly understood.[2,5]

1.1.1 Prognostic Factors: Grade and Stage

Bladder cancer stage is determined according to the tumor-node-metastasis (TNM) system, and is based on the level of progression through the bladder wall. Stage is considered the most important prognostic factor for invasive tumors.[2] A summary of the TNM staging system is shown in Table 1.

Prognosis and management of the disease are guided by histology. Tumors that do not cross the basal lamina to invade the lamina propria (stage Ta, Tis) are referred to as non-muscle-invasive bladder cancer (NMIBC), and are considered to be the least aggressive; tumors that reach the muscle tissue (T2 and above) are categorized as muscle-invasive bladder cancer (MIBC), and are viewed as highly aggressive. Similarly, stage T1 tumors that cross the basal lamina and lamina propria are associated with aggressive disease.[3]

TNM Stage (Primary Tumor)	Description
T0	No evidence of primary tumor
Ta	Papillary carcinoma (non-invasive)
Tis	Carcinoma in situ
T1	Tumor invades connective tissue
T2	Tumor invades muscle
T2a	Superficial muscle
T2b	Deep muscle
T3	Tumor invades perivesical tissue
T3a	Microscopically
T3b	Macroscopically
T4	Tumor invades adjacent structures
T4a	Prostate, uterus, vagina
T4b	Pelvic wall, abdominal wall

Table 1. TNM Stages. Description of tumor stages according to the tumor-node-metastasis system.

Tumor grade is another prognostic factor that is determined by the degree of cellular anaplasia and architectural or cytological atypia. Grade is especially important in prognosticating NMIBC, as it can predict recurrence and progression.[2,6] The most commonly used grading systems are the 1973, 2004, and 2016 WHO grading systems. The 2004 system is generally preferred by pathologists for its simplicity,[2,3] but the 1973 system will be used to describe tumor grade throughout this dissertation due to its superior resolution and the lack of information regarding classification of long-established bladder cancer cell lines using the newer systems. An illustration of the 1973 and 2004 grading systems is shown in Figure 1.[3] Although high-grade tumors are generally more likely to be invasive, it is important to note that bladder cancer stage and grade are independent factors.

Non-invasive tumors can present as high-grade, and invasive tumors can present as low grade, although the latter is considered rare.[6]

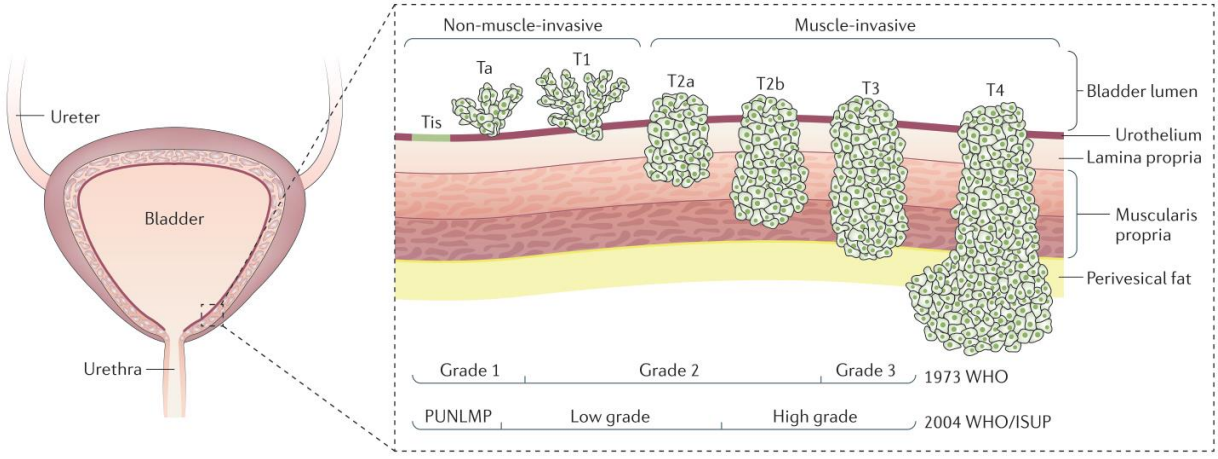

Figure 1. Illustration of tumor stages. Tumor stage and progression through the bladder wall. Approximate correlation between stage and grade showing 1973 WHO and 2004 WHO ISUP grading systems. Source: Sanli, O. et al. Bladder cancer. Nat. Rev. Dis. Prim. 3, 17022 (2017).

1.1.2 Molecular Subtypes of Bladder Cancer

Histological studies and molecular subtyping have revealed that bladder cancer is a complex malignancy with heterogeneous characteristics at the molecular and cellular levels.[3,5,7] Due to the molecular diversity and complexity of the disease, it is challenging to identify which bladder cancer patients are at the greatest risk for disease recurrence and progression and death.[1] Molecular characterization of tumors has the potential to better identify the inherent phenotypic behavior of bladder cancers not entirely captured with standard pathologic analysis. In this regard, several groups have independently completed a molecular characterization of human bladder cancer, leading to the discovery of several transcriptional subtypes of muscle invasive bladder cancer.[8–10] In particular, researchers have identified distinct "luminal" and "basal" subtypes that reflect the hallmarks of breast cancer biology.[10] The luminal subtype exhibits a transcriptional profile with expression patterns similar to those of the normal luminal urothelium. Luminal bladder cancers typically present with the morphology of urothelial carcinoma. In contrast, the basal transcriptional subtype is frequently observed in bladder cancer cells that have undergone

squamous metaplasia (or differentiation). Of these two main subtypes, basal bladder cancer is considered to be significantly more aggressive.[9] While these and other transcriptional subtypes (and associated morphologies) were originally identified at the patient-population level, it is now clear that luminal and basal molecular subtypes can co-exist within an individual tumor.[11,12] However, it is unknown how or if these elements of tumor heterogeneity contribute to disease pathogenesis in general, and invasiveness in particular.

1.2 The Role of NOTCH1-DLL4 signaling in Bladder Cancer

1.2.1 The Notch-Delta Pathway in Humans

The Notch-Delta pathway is a core signaling pathway within the metazoan signaling system that governs tissue morphogenesis, first described in *Drosophila*. The Notch gene encodes a transmembrane receptor for intercellular interaction, and cell fate is thus linked to neighboring cells.[13] In humans, there are four different Notch receptors: NOTCH1, NOTCH2, NOTCH3, and NOTCH4. Notch receptors are activated by the Delta- and Serrate-like (DSL) family of ligands. In humans, there are five such ligands: JAGGED1, JAGGED2, DLL1, DLL3, and DLL4.[14–16] Recently, the Notch pathway has been implicated in cancer progression, including bladder cancer[14,16–18]. NOTCH1 in particular has been found to have a tumor suppressive role in bladder cancer, as the majority of bladder cancers that have been analyzed have NOTCH1 gene copy losses.[17]

Of the DSL ligands, DLL4 has perhaps been the subject of the most research interest due to its suspected role in tumor progression. DLL4 is well known for its role in tip cell formation during angiogenesis[19], but has also been found to regulate leader cell formation during collective cell migration[20]. More recently, DLL4 has emerged as a therapeutic target in cancer, with several research groups promoting DLL4 inhibition as a potential strategy for cancer treatment. However, the role of DLL4 in bladder cancer specifically has not been explored. A simplified illustration of Notch-Delta signaling is shown in Figure 2.[16]

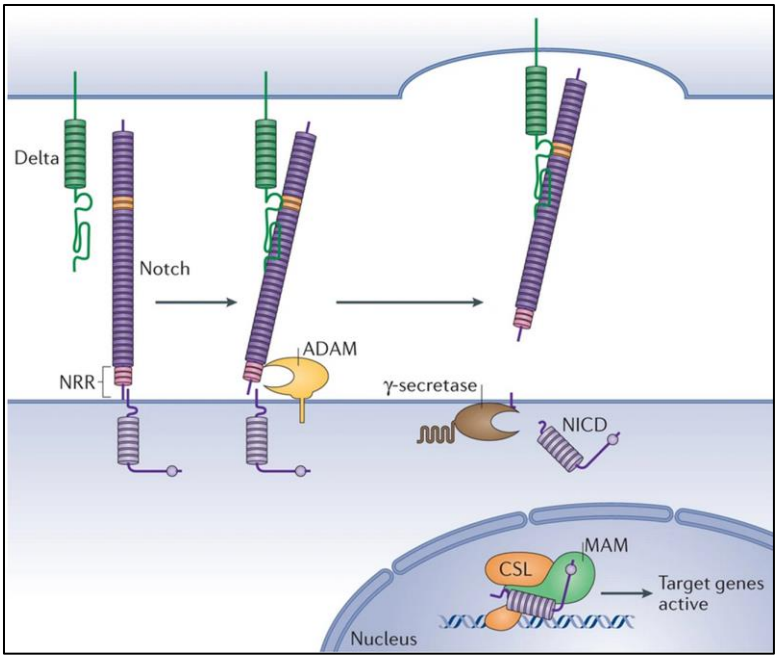

Figure 2. Illustration of Notch-Delta signaling. Interaction between adjacent cells and the Notch intracellular domain (NICD). Source: Bray, S. Notch signalling in context. Nat Rev Mol Cell Biol 17, 722–735 (2016). https://doi.org/10.1038/nrm.2016.94

1.2.2 Modeling Notch-Delta signaling

A simple numerical model of Notch-Delta activation and inhibition by neighboring cells is given by the following set of equations:[21]

$$\frac{dN}{dt} = R_N \frac{D_{in}^k}{a+D_{in}^k} - \mu N \qquad \frac{dD}{dt} = R_D \frac{1}{1+bN^h} - \rho D \qquad D_{in} = \alpha \sum_{cells\ in\ contact} D$$

where N and D refer to intracellular levels of Notch and Delta, RN and RD refer to production rates of notch and delta, and μ and ρ refer to protein degradation rates of Notch and Delta. D_{in} represents the Delta signal from neighboring cells. The function parameters a,b,k,h, the scaling factor α, and production and degradation rates were determined experimentally, and the starting concentrations of intracellular Notch and Delta were randomly generated.[21] Simulation was performed assuming uniform production rates (Figure S1), randomly varying production rates (Figure S2), reduced Notch production (Figure S3), and reduced Delta production (Figure S4). A

summary of the simulation results is shown in Figure 3. The uniform production rate case results in pattern formation due to the lateral inhibition that is characteristic of Notch-Delta signaling.[13] Introducing random variation in both production rates reduced Notch expression in a large number of cells and also led to some variation in Delta expression. Most importantly, the model predicts that inhibiting Notch will increase the number of Delta-expressing cells, whereas Delta inhibition will reduce Notch and Delta concentrations. Similar behavior can be expected regarding NOTCH1-DLL4 signaling in humans.

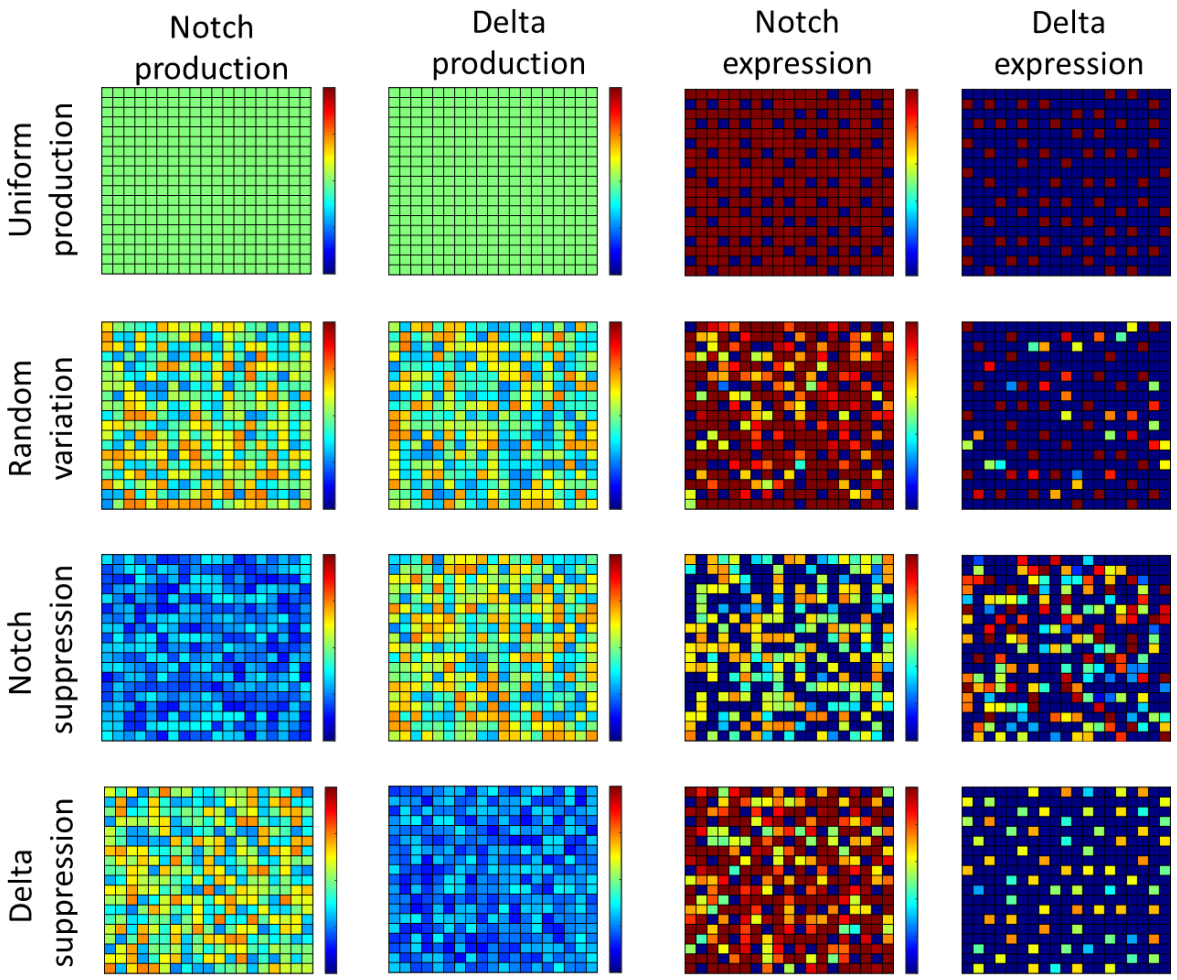

Figure 3. Summary of Notch-Delta Simulation Results. Steady-state Notch and Delta expression patterns are predicted for uniform production rates of Notch and Delta, random variation in production rates, Notch production rate suppression, and Delta production rate suppression. The model consists of a 20 by 20 grid of square cells. Red indicates the greatest expression or production rate, while blue indicates the smallest.

1.3 Experimental Models of Cancer

Recently, 3D organoid models have emerged as a more physiologically relevant alternative to traditional 2D adherent cell models for studying cancer *in vitro*.[22–24] There are several reasons for this trend: 3D models are better suited to mimic the structure of tumors *in vivo*, they preserve the complex cell-cell interactions that take place within solid tumors, and they can also include aspects of tumor interaction with the surrounding microenvironment.[25] An illustration of cancer progression through the surrounding microenvironment is shown in Figure 4.[26] Although this illustration is not specific to bladder cancer, the pattern of progression across the basement membrane and through the stroma, as well as the interaction with stromal cells, is also observed in bladder cancer. Careful consideration must be given to all of these factors when designing a 3D model. All experimental models have limitations, including even the most advanced 3D models.

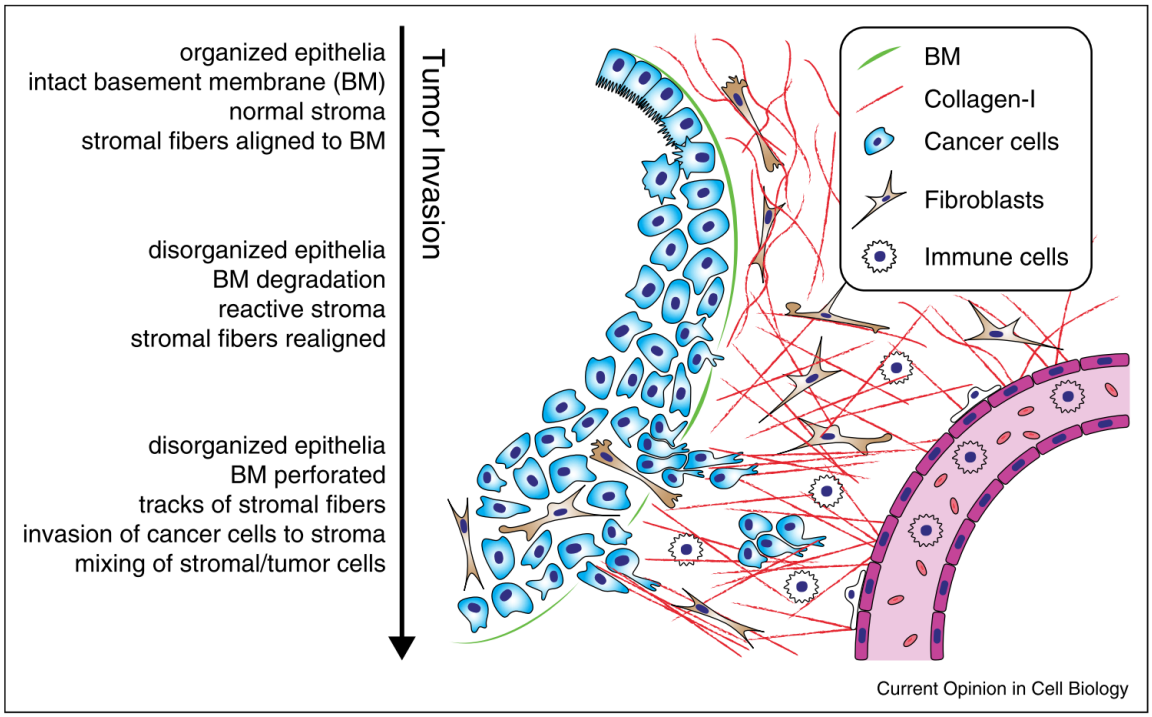

Figure 4. Tumor invasion process. Illustration depicting collective invasion in cancer through the basement membrane (or basal lamina) into the stroma. Source: Clark, A. G. & Vignjevic, D. M. Modes of cancer cell invasion and the role of the microenvironment. Current Opinion in Cell Biology 36, 13–22 (2015).

1.3.1 Characterizing Cancer Invasion

Several approaches have also been developed to study tumor cell invasion through the extracellular matrix (ECM) *in vitro*. These approaches include spheroid sprouting assays,[27] modified Boyden chambers,[28,29] and microfluidic culture systems.[30] Nevertheless, conventional invasion assays often focus on the invasion of cancer cells at the population level and pay little attention to the behaviors of subpopulations and individual cells within a given population. The influence of cellular and molecular heterogeneity on bladder cancer invasion remains poorly understood. Furthermore, the collective invasion mechanisms, such as the formation of invasive leader cells,[31] have not been investigated systematically in bladder cancer.

1.3.2 Spatiotemporal Dynamics of Gene Expression

The investigation of 3D tumor invasion is further hampered by the lack of effective approaches to dynamically monitor gene expression in live cells within 3D microenvironments. This is particularly challenging for characterizing the molecular diversity in human primary culture cells from patient-derived tumor samples. The inability to study spatiotemporal dynamics of gene expression, therefore, has limited the investigation of the invasion mechanisms and prevented the discovery of therapeutic targets that would allow innovation in the clinical management of this common disease.

1.4 Research Overview

The purpose of this research is to develop an experimental model to characterize the invasive potential of bladder cancer cells for eventual use in research and personalized medicine applications. Toward personalized medicine, such a model would serve as a phenotypic surrogate assay - allowing pathologists to quickly assess the invasive potential of cells derived from patient tissue samples and even test different treatment strategies, which would improve treatment outcomes. In this research, the invasion assay is used to study the mechanism behind collective invasion in bladder cancer microtumors within a physiologically relevant 3D microenvironment,

demonstrating its compatibility with single-cell gene expression analysis, pharmacological perturbation, and transient knockdown experiments. The specific objectives are as follows:

1. Design and optimize an extracellular matrix (ECM)-based model of the bladder stratified urothelium, including the basal lamina and lamina propria, that accurately recapitulates tumor grade and progression (stage) *in vitro*. The experimental model should be compatible with established immortal bladder cancer cell lines and primary culture cells derived from patient tumor samples.
2. Investigate established human bladder cancer cell lines representing basal and luminal subtypes, and characterize invasive subpopulations in detail. Examine the role of NOTCH1-DLL4 signaling in microtumor invasion.
3. Generate co-culture microtumors, composed of multiple cellular subtypes, to study the heterotypic interaction between basal and luminal subtypes within bladder cancer tumors and the corresponding effects on tumor progression. Examine the role of NOTCH1-DLL4 signaling in basal-luminal interaction, and explore the role of the lumial marker FOXA1.

Chapter 2

Invasion Assay Development

2.1 A Bladder Cancer Specific Invasion Assay

A primary goal of this research is the development of a bladder cancer specific invasion assay that recapitulates key features of bladder cancer tumors *in vivo* and also mimics the bladder microenvironment. This experimental model should be compatible with confocal laser-scanning microscopy (CLSM) and GNR-LNA biosensors for simultaneous analysis of microtumor invasion and single-cell gene expression. Furthermore, the assay should be compatible with traditional microbiological techniques such as drug perturbation and RNA interference to be effective as a screening platform for personalized medicine.

2.1.1 Re-Creating Bladder Tissue *in vitro*

When developing an experimental model to represent something as complex as bladder physiology, it is important to focus on aspects that are most relevant to the problem under consideration. At a high level, the bladder wall consists of several layers: the stratified urothelium, composed of layers of epithelial cells; the basement membrane, a thin layer of ECM secreted by cells that serves as a significant barrier to invasion; the lamina propria, a thicker layer of ECM that also contains fibroblasts and blood microcapillaries; bladder wall muscles, referred to as the muscularis propria; and the perivesical fat layer.[1,3,32,33] One of the most important distinctions affecting bladder cancer prognosis is that between MIBC and NMIBC. Therefore, a physiologically relevant model for bladder cancer should include both ECM layers between the urothelium and the muscularis propria. It is reasonable to assume that a tumor capable of progressing through these layers has the potential to reach the muscularis propria, which would distinguish MIBC from NMIBC and therefore be useful in the initial assessment of a patient tumor sample. An illustrated cross-section of the bladder wall is shown in Figure 5.[33]

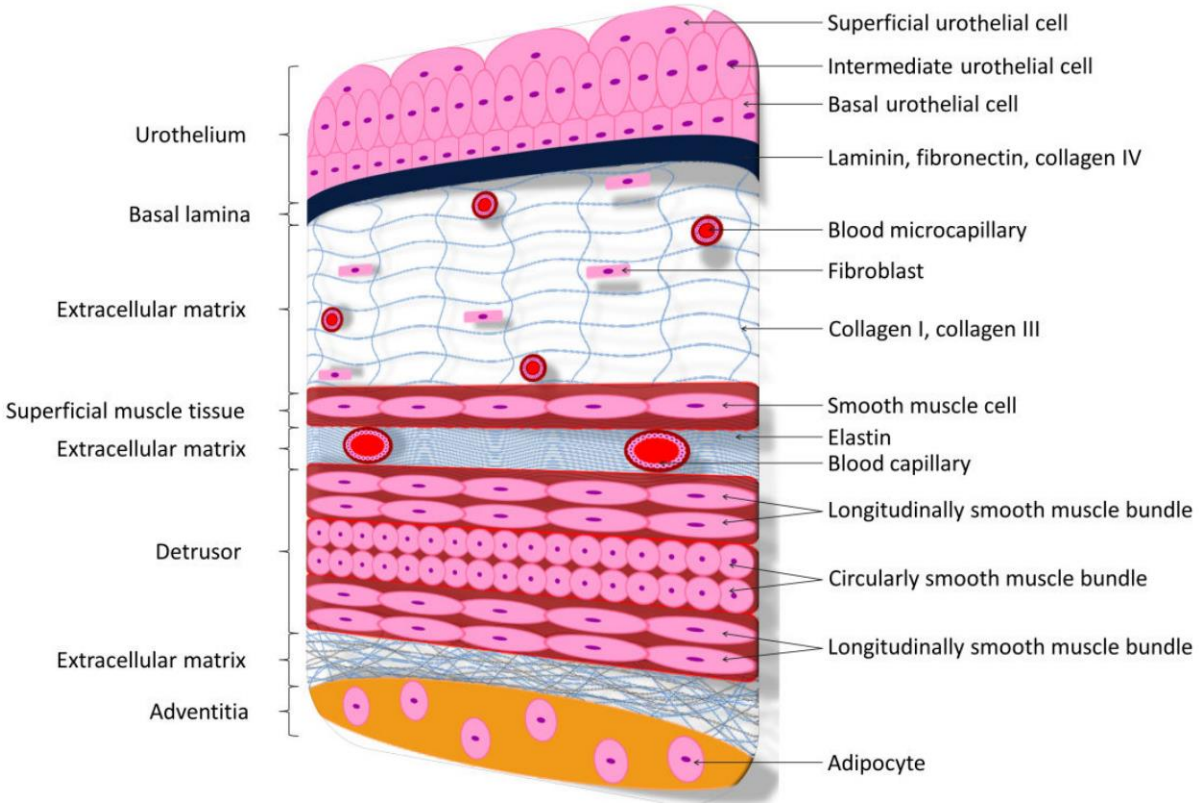

Figure 5. The bladder wall. Cross-section view of bladder wall with labeled layers and composition. Note: the lamina propria is simply referred to as extracellular matrix in this figure. Source: Sara Bouhout, Alexandre Rousseau, Stéphane Chabaud, A. M. and S. B. Potential of Different Tissue Engineering Strategies in the Bladder Reconstruction. in Regenerative Medicine and Tissue Engineering doi:http://dx.doi.org/10.5772/55838

2.1.2 Generating Multifocal Bladder Cancer Tumors

Researchers have described a multifocal, metachronous development pattern for bladder cancer tumors.[34] Some have proposed that the cause of this is due to a defect in the entire bladder urothelium that makes it susceptible to tumorigenesis under the right environmental conditions[35]; others suggest that cancer cells simply spread from the primary tumor to other locations within the urothelium.[34–37] In either case, the multifocal nature of bladder cancer tumors is a unique characteristic that should be included in an experimental model that is disease specific. This is especially important for studying collective invasion mechanisms, which by definition require coordination between cells. Creating multifocal bladder cancer microtumors within the

experimental model has the added advantage of producing a large number of samples to analyze, which in turn reveals invasive subpopulations even when invasion occurs infrequently.

2.2 Design and Optimization of Experimental Model

Although ECM-based experimental models of cancer are becoming increasingly common in research, there is currently no such model that specifically mimics the key aspects of bladder cancer described in the previous section. To address this problem, ECM properties were optimized to create a physiologically relevant experimental model of bladder cancer representing the urothelium, basal lamina, and lamina propria. A self-assembly process was optimized for bladder cancer cells and was then used to generate multifocal bladder cancer microtumors on top of basal lamina ECM. In preliminary experiments, a simplified model representing only the basal lamina was used to screen all available bladder cancer lines for their potential to breach this membrane, which is a critical first step in tumor progression.[38] Preliminary results using the simplified model to study collective invasion and perturbation of the NOTCH1-DLL4 signaling pathway are discussed in Chapter 3. The full model, representing the basal lamina and lamina propria, consisted of two distinct types of ECM, each of which had to be optimized for reliable solidification and consistent properties with minimal solidification time. A detailed study of heterotypic interaction among cell subpopulations and the role of NOTCH1-DLL4 signaling using the full model is discussed in Chapter 4.

2.2.1 The Simplified Model and Microtumor Self-Assembly Process

A self-assembly process was developed to generate a large number of bladder cancer microtumors on the top layer of ECM which represents the basal lamina. The process was adapted from a technique used previously for breast cancer cells[39] and optimized for bladder cancer cells and basal lamina specific ECM. Growth factor reduced Matrigel (Corning) was diluted to 8 mg/mL in chilled, complete culture medium (Corning). Fluorescent beads (Spherotech) were then added at a volume ratio of 1:10,000 to label the Matrigel for imaging. 40 µL labeled Matrigel was applied to each well of a chilled glass-bottom 96-well plate (CellVis), which was then placed in a humidified cell incubator at 37°C, 5% CO_2 for 30 min to solidify. Cells were then detached using

0.25% trypsin, 0.53 mM EDTA solution (Corning), suspended in complete culture medium at a concentration of 10^6 cells/mL, and seeded atop the solidified Matrigel at a concentration of 10^4 cells per well. The plate was then covered and returned to the cell culture incubator for 3 days before imaging. The concentration of Matrigel was determined based on the manufacturer's recommendations and a review of current invasion assays using Matrigel. The solidification time and cell seeding density were optimized to produce the maximum number of separate spheroids. Optimization of the solidification time and seeding density is shown in Figure 6.[40]

2.2.2 Optimization of Full Multilayer Model

The incorporation of simulated lamina propria ECM into the full, multilayer model presented several challenges that required significant fine-tuning to reliably produce distinct, stratified layers. Collagen type 1 is the primary component of the lamina propria, so collagen 1 gel from rat tail was used to represent this layer. The polymerization and resulting microstructure of collagen 1 are dependent on several factors: protein concentration, pH, ionic strength (salt concentration), and polymerization temperature.[41–44] There are limitations associated with all of these factors. Protein concentration is perhaps the easiest property to adjust, and has a significant effect on the bulk mechanical properties and microstructure of collagen 1.[41] In practice, commercially available collagen 1 can vary in protein concentration from 3.5-4.0 mg/mL, and based on experience, it cannot reliably form a solid gel at concentrations below 1.0 mg/mL. An intermediate protein concentration of 2.0mg/mL was selected based on well-characterized mechanical properties and microstructure at this concentration.[41,43] Furthermore, this concentration was found to be most suitable for bladder cancer microtumor growth in preliminary tests, and collagen 1 concentrations between 2.0-2.5mg/mL are the most widely used in cancer invasion assays.

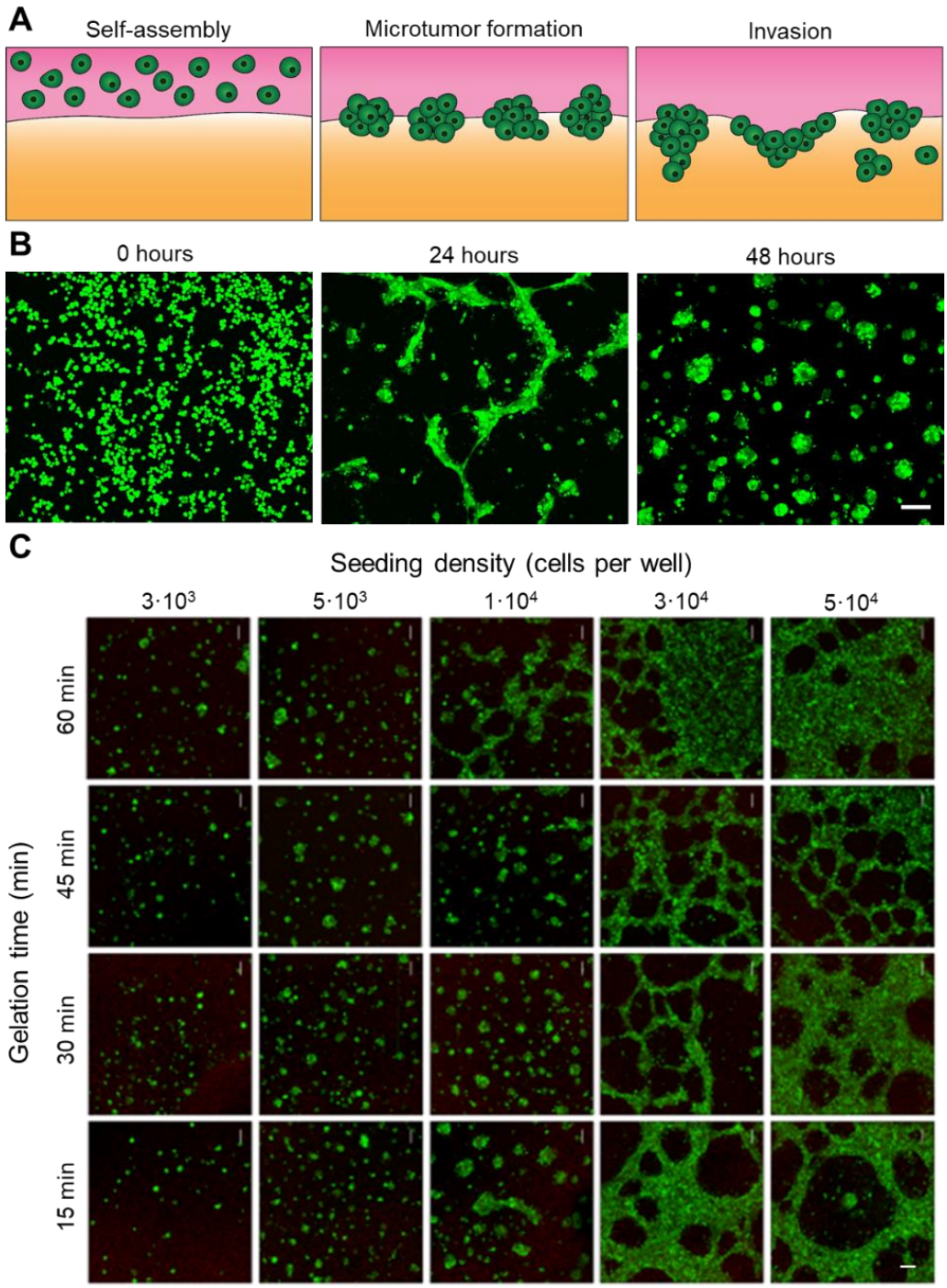

Figure 6. Microtumor self-assembly on Matrigel substrate. (A) Illustration of self-assembly followed by invasion. (B) Microtumor formation during the first 48 hours after cell seeding. (C) Effect varying incubation time and cell seeding density (96 well plate, surface area approximately 0.32 cm^2) for Matrigel 8 mg/mL in complete culture medium (MEM). Scale bars: 50µm. Source: Torab, P. et al. Three-Dimensional Microtumors for Probing Heterogeneity of Invasive Bladder Cancer. Anal. Chem. 92, 8768–8775 (2020).

The development of the full, multilayer model also required re-optimization of the basal lamina layer. The purpose of this was to reduce the thickness of this layer as much as possible to better mimic the basal lamina in vivo, and also to account for the substrate change from chilled glass to collagen 1 at 37°C. To accommodate these changes, Matrigel was diluted to a protein concentration of 5mg/mL, and the amount was reduced to 10µL per well.

2.2.3 Assembling the Full Model

Collagen type 1 from rat tail (SigmaAldrich) at a starting concentration of 4mg/mL was diluted to 2mg/mL in complete culture medium (Corning), and neutralized using 1M NaOH to a final pH of 7.75. The final concentration of fetal bovine serum (FBS, Corning) was 20%. 40µL of collagen 1 was added to each well of a chilled glass-bottom 96-well plate (CellVis), which was then placed in a humidified cell incubator at 37°C, 5% CO_2 for 60 min to solidify. Solidification was confirmed by visually inspecting for turbidity. Growth factor reduced Matrigel (Corning) was diluted to 5 mg/mL in chilled, complete culture medium (Corning). Fluorescent beads (Spherotech) were then added at a volume ratio of 1:10,000 to label the Matrigel for imaging. 10 µL labeled Matrigel was then carefully applied to each well on top of the solidified collagen 1 layer, and the entire 96-well plate was then returned to the cell incubator for 15 min to solidify. Cells were detached using 0.25% trypsin, 0.53 mM EDTA solution, and suspended in complete culture medium at a concentration of 10^6 cells/mL, then seeded atop the solidified Matrigel layer at a concentration of 10^4 cells per well.

2.3 Cell Culture

2.3.1 Culture of Established Urothelial Cancer Cell Lines

The bladder cancer cell lines RT4, UM-UC-3, SCaBER, HT-1197, HT-1376, and 5637 were obtained from ATCC, and UM-UC-1 was obtained from Sigma-Aldrich. Upper tract urothelial carcinoma cell lines CRL-9520 and UM-UC-14 were obtained from ATCC and Sigma-Aldrich, respectively. RT4 cells were maintained in McCoy's 5A culture medium, CRL-9520 was maintained in F-12K, and all other cell lines were maintained in MEM with 2 mM glutamine

(Corning). Culture medium for HT-1197 and HT-1376 was supplemented with 1x non-essential amino acids and 1 mM sodium pyruvate (Gibco). All culture media were supplemented with 10% fetal bovine serum (Corning) and 1 μg/mL Gentamicin (Gibco). The effects of cell culture media on invasion were not considered in this study. Cells were grown in 60 mm tissue culture dishes and were incubated at 37°C, 5% CO2 with 95% humidity. The cells were examined under a microscope on a daily basis, and the medium was renewed every 2 days. Cells were passaged at 70% confluence using 0.25% trypsin, 0.53 mM EDTA solution (Corning).

2.3.2 Human Primary Tumor Cells Derived from Patient Samples

The procedure was approved by the Pennsylvania State University Institutional Review Board (PSU IRB# STUDY00008190). Following informed consent, tissue was collected and stored in Dulbecco's Modified Eagle Medium (DMEM; Gibco) containing 50 μg/mL Gentamicin (Sigma), and gently scraped to liberate urothelial cells. The cell suspension was combined with an equal volume of Optiprep Density Gradient Medium (30%; Sigma). Following thorough mixing, cells were overlaid with keratinocyte serum-free growth medium (KSFM; Gibco) and centrifuged at 800 x g for 15 minutes at 4 degrees C in a Sorvall ST8R refrigerated centrifuge (Thermo Scientific). Interphase containing urothelial cells was transferred to a 15 ml conical vial (Falcon) containing KSFM. This cell suspension was subsequently centrifuged. Following aspiration of the supernatant, the cell pellet was suspended in KSFM growth medium at a plating density between 10,000 and 50,000 cells/cm2.

2.3.3 RNA Interference and Pharmacological Treatments

DAPT was obtained from Sigma-Aldrich; DLL4, NOTCH1, and non-targeting control siRNA were purchased from Santa Cruz Biotech. DAPT was dissolved in DMSO and diluted in medium to desired concentrations for drug response testing. DAPT was added after microtumor self-assembly, 48 hours before imaging. All siRNAs were diluted in serum-free medium and mixed with Hiperfect transfection reagent (Qiagen) according to the manufacturer's instructions. Transfection was performed in monolayer culture for 24 hours prior to microtumor self-assembly. An siRNA concentration of 30pM was used for all RNA interference experiments, based on

manufacturer instructions and experience. Probes were incubated for 10 minutes at room temperature with MUTAB-coated GNRs (Nanopartz) with 10 nm diameter and 29 nm length. Cells were incubated overnight with GNR-LNA probe complex to allow sufficient time for cellular uptake. After incubation, cells were washed three times with PBS 1x to remove excess GNR-LNA probe complex.

2.3.4 GNR-LNA Probe Preparation and Treatment

GNR-LNA probes were used to detect single cell level DLL4 mRNA and NOTCH1 mRNA expression within the microtumors. LNA probes labeled with Texas Red or Alexa Fluor 647 were obtained from Integrated DNA Technologies. Probes at a concentration of 15nM were prepared in 1x Tris-EDTA buffer. Probes were incubated for 10 minutes at room temperature with 4μL MUTAB-coated GNRs (Nanopartz) with 10 nm diameter and 29 nm length. Cells were incubated for 12 hours in normal conditions (described in Section 2.3.2) with GNR-LNA probe complex to allow sufficient time for cellular uptake.

2.3.5 Cell Staining

Cells were stained using CellTracker Green CMFDA (Invitrogen) at a concentration of 20 μM in PBS for 30 minutes, then washed three times with PBS 1x. Cells were left to recover in complete culture medium for at least 3 hours before detaching for spheroid formation. For co-culture experiments, one cell line was stained with CellTracker Red CMTPX to distinguish between different cell types within an image stack. Cell stains were alternated in experimental repeats to account for effects of different stains, but no such difference was observed.

2.4 Data Processing

2.4.1 Imaging

3D images stacks were acquired using confocal microscopy (Leica SP8) and reconstructed using open-source software (NIH ImageJ). Images were taken 72 hours after cell seeding and every 48

hours afterwards for a total of three imaging sessions. The first image set was used for biosensor fluorescence measurements in all experiments, and the first or third set was used to analyze invasion depth, as indicated in figure captions. Invasion depth was measured as the distance from the gel-medium interface to the leading edge of each spheroid. To analyze fluorescence intensity, 3D images containing individual spheroids were imported into MATLAB and binarized, and intensity was calculated as the ratio of active pixels for the probe channel to the number of active pixels for the cell stain channel. This method provides an estimate of fluorescence intensity that accounts for the number of cells present in an image.

2.4.2 Statistical Analysis

Invasiveness and DLL4 mRNA expression were compared between experimental groups using appropriate non-parametric tests as specified in figure captions, mainly the Kruskal-Wallis test for comparing between-group and within-group variance and the Wilcoxon Rank Sum test for comparing medians of two groups. Non-parametric tests were chosen due to the non-normal distribution of most depth data. Two-sample t-tests were used to analyze some results that were assumed to have a normal distribution, as indicated in figure captions. Statistical analysis was performed using MATLAB statistics toolbox (Mathworks). A p value less than 0.05 was considered statistically significant. The following abbreviations are used to denote p value throughout this dissertation: *$p<0.05$, **$p<0.01$, ***$p<0.001$.

Chapter 3

Investigating Bladder Cancer Invasion Using Simplified Model

3.1 Results

3.1.1 Urothelial Carcinoma Cells Self-Organize into Microtumors

Urothelial carcinomas of the kidney, ureter, and bladder are characterized by the tendency of the tumor being confined in the mucosa or invading through the basement membrane (primary tumor stages Tis and pTa) and lamina propria (stage T1) and eventually into the muscularis propria (stage T2) as shown in Figure 1. To mimic the lumen-tumor-basal lamina structure, the previously described simplified ECM model was utilized. The cancer cells migrated and aggregated on the ECM to form microtumor structures as shown in Figure 6. Hundreds of microtumor structures could be developed simultaneously with an appropriate cell seeding density and ECM properties. The tumor-on-gel self-assembly was implemented in standard 96-well plates. The microtumor assay is compatible with bladder cancer cells and other urothelial carcinoma cells. In addition to spheroid-like invasive microtumors, flat carcinoma and papillary carcinoma-like microtumors with infiltrative and finger-like protrusions that recapitulate the diversity of bladder cancer invasion were observed, as shown in Figure 7.

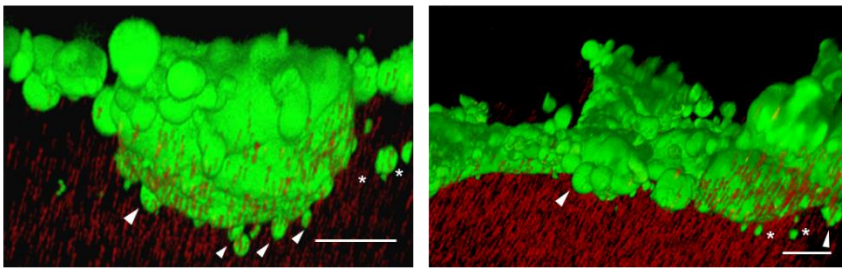

Figure 7. 3D reconstruction of microtumors. 3D reconstruction of urothelial carcinoma cells (green) on a Matrigel substrate (red) using NIH ImageJ, with sprouts indicated by white arrowheads and detached cells by white asterisks. Scale bars: 50µm. Source: Torab, P. et al. Three-Dimensional Microtumors for Probing Heterogeneity of Invasive Bladder Cancer. Anal. Chem. 92, 8768–8775 (2020).

3.1.2 Invasion of Bladder Microtumors with Heterogeneous Characteristics

Bladder cancer cell lines with luminal (UM-UC-1 and RT4) and basal (HT-1376) molecular signatures as well as a highly invasive bladder cancer cell line (UM-UC-3, which is not classified as either luminal or basal) were investigated to study the microtumor invasion model (Figure 8).[45] Microtumors were allowed to form and invade the ECM for 72 hours. Confocal imaging with 3D reconstruction was performed to visualize the invading microtumors and estimate the invasion depth (Figure 8D). For cell types with a luminal signature, such as UM-UC-1 (grade 2) and RT4 (grade 1-2),[46] the microtumors had a low-to-medium tendency to invade Matrigel, which is composed of basement membrane matrix. In contrast, HT-1376 (grade 3)[46] exhibited significantly higher invasiveness than UM-UC-1 and RT4. Furthermore, UM-UC-3 displayed highly aggressive behavior, with invading sprouts and detached cells and cell clusters from the microtumors.

The distribution of invasion depth was analyzed for several bladder cancer cell lines (Figure 8D, Supplementary Figure S5). UM-UC-1 microtumors did not display any observable invasiveness beyond contact mechanics.[47] In contrast, the other cell lines displayed substantial heterogeneity in the invasive behaviors. A small portion of RT4 microtumors invaded over 100 μm while the majority of microtumors invaded less than 50 μm. Data analysis suggests a distorted Gaussian distribution or a bimodal distribution, implying a heterogeneous subpopulation of cancer cells may exist among the microtumors formed by the individual cell line. Similarly, small subpopulations of HT-1376 microtumors appeared capable of invading the ECM with higher frequency than the luminal cell lines. The majority of UM-UC-3 microtumors were highly non-spheroidal and invasive. For the cell lines HT-1376 and UM-UC-3, both the frequency of invading microtumors and the invasion depths were increased, representing a spectrum of invasiveness among these cell lines. These results are in excellent agreement with previous investigations of bladder cancer cell behaviors using in vivo and ex vivo bladder cancer models.[46,48–50]

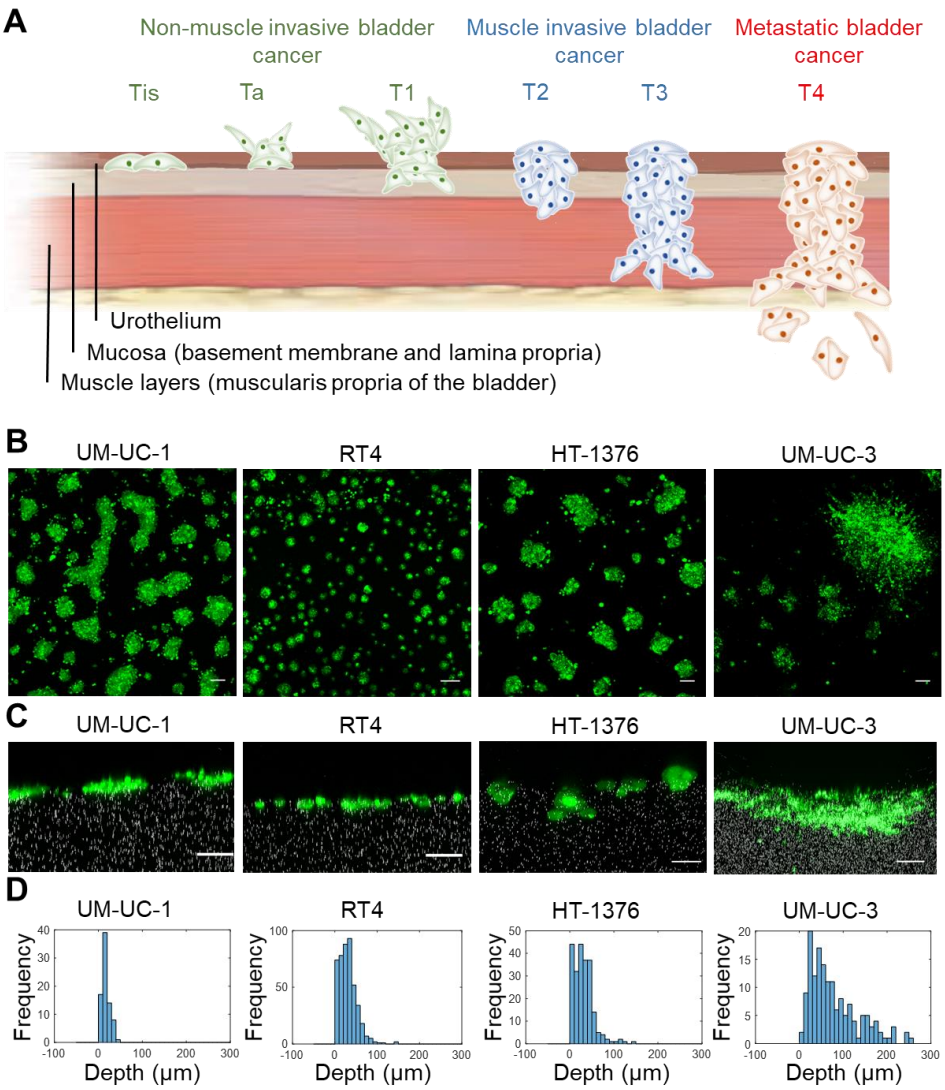

Figure 8. A microtumor model for probing bladder cancer invasion. (A) Illustration of tumor stages. (B) Vertical projection view of 3D microtumors generated from various cell lines. (C) Horizontal projection cross-section views of microtumors. (D) Histograms of invasion depth. Combined results of 3 independent experiments. Scale bars: 50μm. Source: Torab, P. et al. Three-Dimensional Microtumors for Probing Heterogeneity of Invasive Bladder Cancer. Anal. Chem. 92, 8768–8775 (2020).

3.1.3 Analysis of DLL4 Expression in Invading Microtumors using the GNR-LNA Biosensor

Next, the invasion mechanism of microtumors was measured using a GNR-LNA biosensor. In particular, the expression of DLL4 mRNA was studied as it is associated with the formation of leader cells during epithelial wound healing.[20,51] The GNR-LNA biosensors were internalized by

the cells and detected the target mRNA by the displacement reaction between the target mRNA and the GNR (Figure 9A).[52–54] When used in combination with 3D confocal imaging, this biosensor allows us to study the spatiotemporal distribution of mRNA expression within individual microtumors. An LNA sequence for targeting DLL4 mRNA was previously designed and optimized.[55] Probe sequences targeting β-actin and GAPDH mRNA were included as the positive control, and a random sequence was chosen as the negative control.[18,27] In the experiment, β-actin and GAPDH probes exhibited little variation in the volume average expression among the microtumors, and the expressions were also relatively uniform within individual microtumors (Figure 9B). The random probes, in contrast, maintained a low background signal. Interestingly, the bulk expression of DLL4 was heterogeneous among different microtumors, and non-uniform distribution of DLL4 expression was observed within some of microtumors (Figure 9B). Specifically, cells displayed a high level of DLL4 mRNA at the leading front in some microtumors. These results suggest DLL4 is spatially coordinated in bladder microtumors.

3.1.4 NOTCH1-DLL4 Signaling is Involved in Collective Invasion of Bladder Cancer Cells

The expression of DLL4 mRNA has been associated with the formation of leader cells in epithelial wound healing and endothelial tip cells during angiogenesis.[20,51,56,57] To study the role of DLL4 in the formation of invasive leader cells and bladder cancer invasion, 3D reconstruction was applied to evaluate the DLL4 expression in invading microtumors. HT-1376, which has a moderate invasiveness and form uniform spheroids, was chosen as the model cell. The expression of DLL4 mRNA was upregulated in HT-1376 cells at the leading front of invading microtumors (Supplementary Figure S6). To characterize this observation, the level of DLL4 was measured at day 3 after cell seeding and the migration of microtumors was tracked over the following 72 hours. Microtumors with a high level of DLL4 at the leading front generally invaded a greater depth compared to microtumors with a low level of DLL4 (Supplementary Figure S6A). The data revealed a positive correlation between the level of DLL4 at the leading front and invasion depth, supporting a role of DLL4 in bladder cancer invasion.

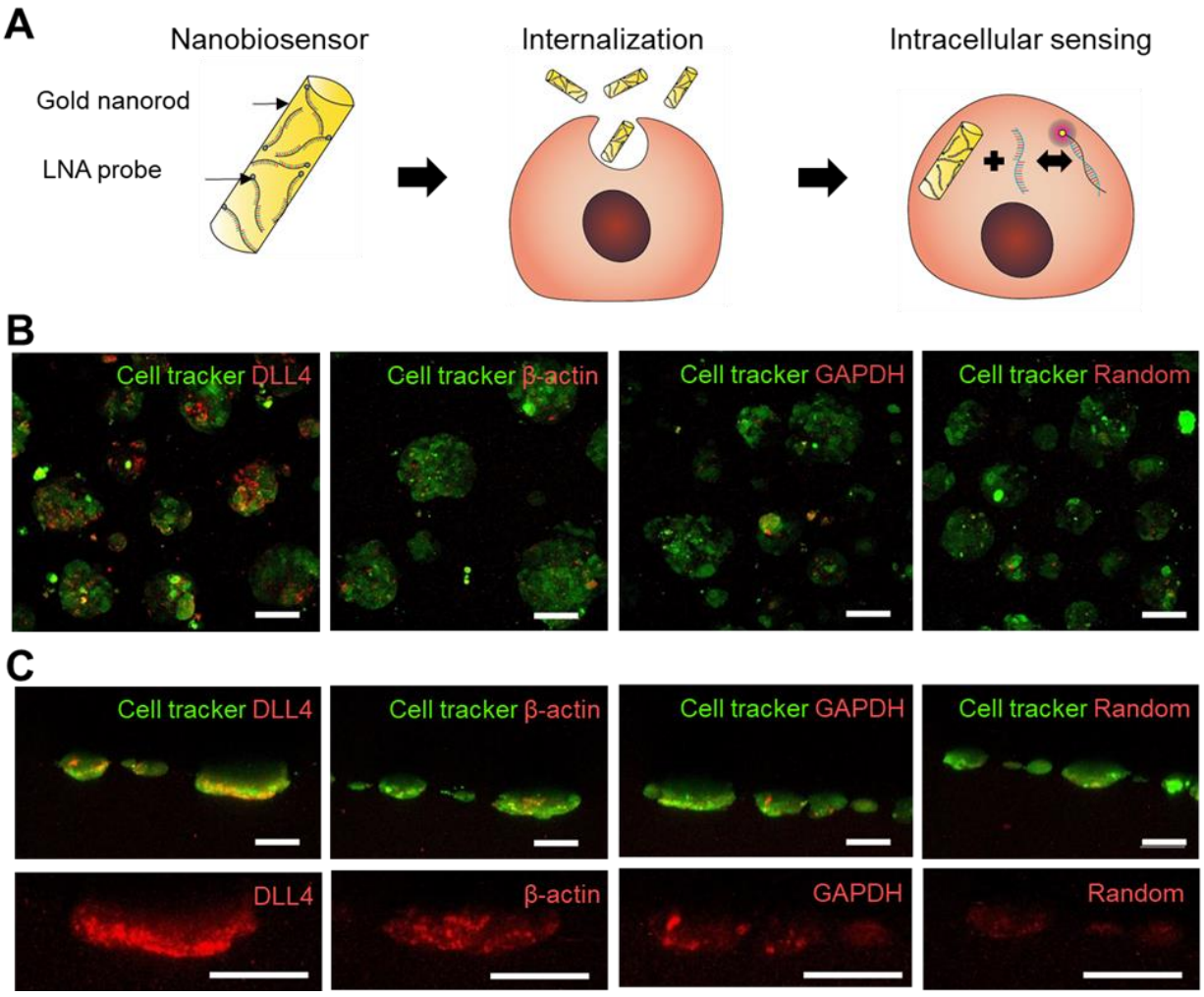

Figure 9. A gold nanorod-locked nucleic acid (GNR-LNA) biosensor for gene expression analysis in 3D microtumors. (A) Illustration mRNA detection using GNR-LNA biosensor. (B) Vertical projection view of 3D microtumors (green) showing biosensor signal (red) for DLL4 sensor along with positive (β-actin, GAPDH) and negative (Random) control sensors. (C) Horizontal projection cross-section views of microtumors showing biosensor signal. (D) Detail view of biosensor signal revealing spatial expression profiles. Scale bars: 50μm. Source: Torab, P. et al. Three-Dimensional Microtumors for Probing Heterogeneity of Invasive Bladder Cancer. Anal. Chem. 92, 8768–8775 (2020).

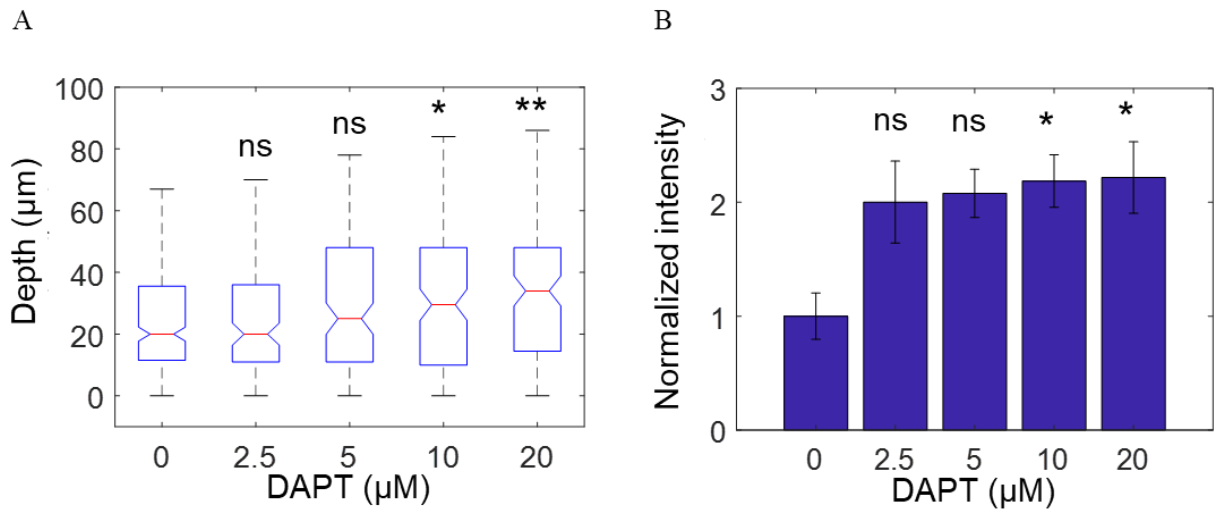

Figure 10. Effect of DAPT on HT-1376 invasion and DLL4 expression. (A) Invasion depth of HT-1376 cells exposed to various concentrations of DAPT (B) Average DLL4 expression based on fluorescence intensity, normalized relative to control group. *p<0.05, **p<0.01 (Kruskal-Wallis one-way ANOVA with Tukey-Kramer post test). Source: Torab, P. et al. Three-Dimensional Microtumors for Probing Heterogeneity of Invasive Bladder Cancer. Anal. Chem. 92, 8768–8775 (2020).

NOTCH1 is a receptor of DLL4 and is associated with the progression of bladder cancer.[58] In particular, NOTCH1 is suggested as a tumor suppressor, and inhibition of NOTCH1 signaling promotes bladder cancer progression.[14,17] Therefore, the influence of NOTCH1-DLL4 signaling on the invasion of bladder microtumors was investigated. HT-1376 microtumors were treated with DAPT, a γ-secretase inhibitor, which prevents the cleavage of the Notch intracellular domain and therefore inhibits Notch activation. HT-1376 cells were treated with DAPT prior to microtumor self-assembly. Upregulation of DLL4 was observed in microtumors treated with DAPT (Figure 10B). This observation is consistent with the inhibitory role of NOTCH1 on DLL4.[59] Interestingly, invasion depth measurements indicated that increasing concentrations of DAPT increased the median invasion depth (Figure 10A).

The effect of NOTCH1-DLL4 signaling on bladder cancer invasion was further investigated by RNA interference. HT-1376 cells were treated with NOTCH1 and DLL4 siRNA before seeding, and microtumor invasion was monitored in the same manner. In agreement with the DAPT data, transient knockdown of NOTCH1 enhanced the expression of DLL4 (Figure 11B) and increased

the invasion depth (Figure 11A). In contrast, DLL4 siRNA reduced DLL4 expression (Figure 11B) and significantly attenuated the invasion of microtumors relative to control siRNA (Figure 11A). These results collectively support the inhibitory role of NOTCH1 on DLL4 expression and bladder tumor invasion.

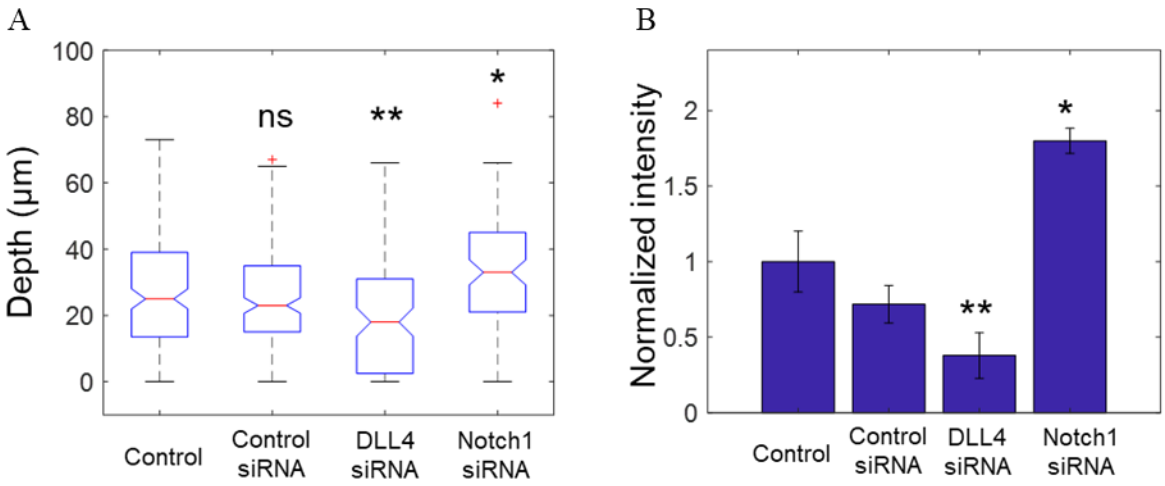

Figure 11. Effect of transient knockdown on HT-1376 invasion and DLL4 expression. (A) Invasion depth of HT-1376 cells treated with siRNA (B) Average DLL4 expression based on fluorescence intensity, normalized relative to control group. *p<0.05, **p<0.01 (Kruskal-Wallis one-way ANOVA with Tukey-Kramer post test). Source: Torab, P. et al. Three-Dimensional Microtumors for Probing Heterogeneity of Invasive Bladder Cancer. Anal. Chem. 92, 8768–8775 (2020).

3.1.5 Characterization of Patient Derived Primary Tumor Cells

To evaluate the involvement of DLL4 in patient samples and demonstrate personalized analysis using the 3D microtumor invasion assay, fresh human clinical specimens collected from patients diagnosed with bladder cancer were incorporated. A protocol for studying patient-derived tumor cells was optimized for these specimens[60,61], and the invasiveness of the sample was functionally characterized. As with established cell lines, the primary cells were stained and the GNR-LNA biosensor targeting DLL4 mRNA was applied for single cell gene expression analysis. Submicron

fluorescent particles were embedded in the ECM to track the invasion depth of the microtumor. Figure 12 shows a microtumor generated by a high-grade papillary urothelial carcinoma sample obtained from TURBT. Similar to the experiments using bladder cancer cell lines, the primary cancer cells self-assembled on the ECM. The cells formed a single microtumor of ~500 μm diameter in each well, and the morphology of the microtumor was similar to the high-grade UM-UC-3 cells (Figure 8). Some of the cells invaded aggressively as protruding structures sprouting from the microtumor (Figure 12D). The microtumor also exhibited many small aggregates detaching and penetrating collectively and individually into the ECM over time (Figure 12E). In agreement with the experiments using cell lines, DLL4 expression was upregulated in both the main microtumor and detached cell aggregates. The distribution of DLL4 was non-uniform among the aggregates (Figure 12E, Figure 13). In particular, the majority of invading cell aggregates had one or more DLL4 expressing cells while the other cells in the aggregate exhibited a low or undetectable level of DLL4 mRNA. The average DLL4 expression is comparable between cells at the boundary of the main spheroid and the detached cell aggregates (Figure 13B). Interestingly, the invasion depth of cell aggregates with DLL4 expressing cells (n=13) is significantly higher than cell aggregates without (n = 4) DLL4 expressing cells (Figure 13C). These results further support the correlation between increased DLL4 expression and invasive behavior and demonstrate the importance of molecular heterogeneity within a tumor sample.

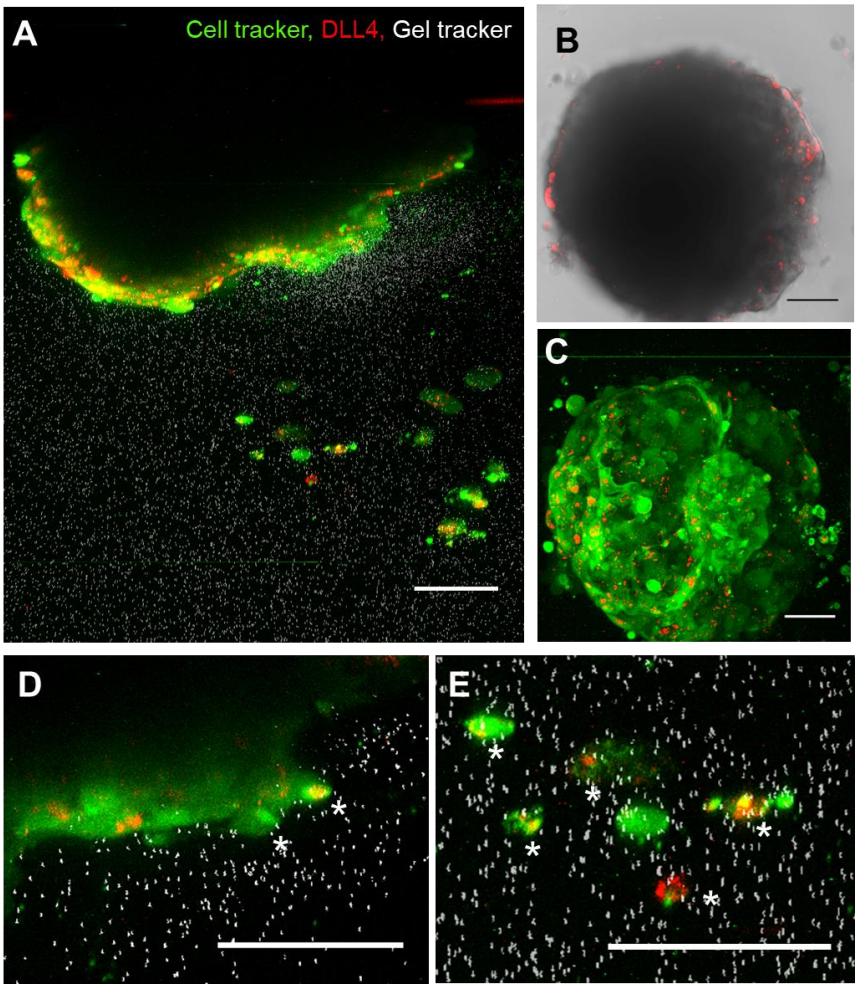

Figure 12. Invasion of patient-derived primary tumor cells. (A) Invasion of cancer cells (cross-sectional view) from a high-grade papillary urothelial carcinoma sample obtained from transurethral resection. Fluorescent particles (white) were embedded in the ECM, and cells were stained with a CellTracker dye (green) and the GNR-LNA biosensor targeting DLL4 mRNA (red). (B-C) Bright-field and fluorescence images (top view) of the microtumor. (D-E) Zoomed-in views of cancer cells in the main microtumor and detached cells or aggregates. Red color indicates DLL4 expression in invading cells. White asterisks indicate leader cells protruding out from the microtumor structure and invading aggregates with DLL4 expressing leader cells. Scale bars, 100μm. Source: Torab, P. et al. Three-Dimensional Microtumors for Probing Heterogeneity of Invasive Bladder Cancer. Anal. Chem. 92, 8768–8775 (2020).

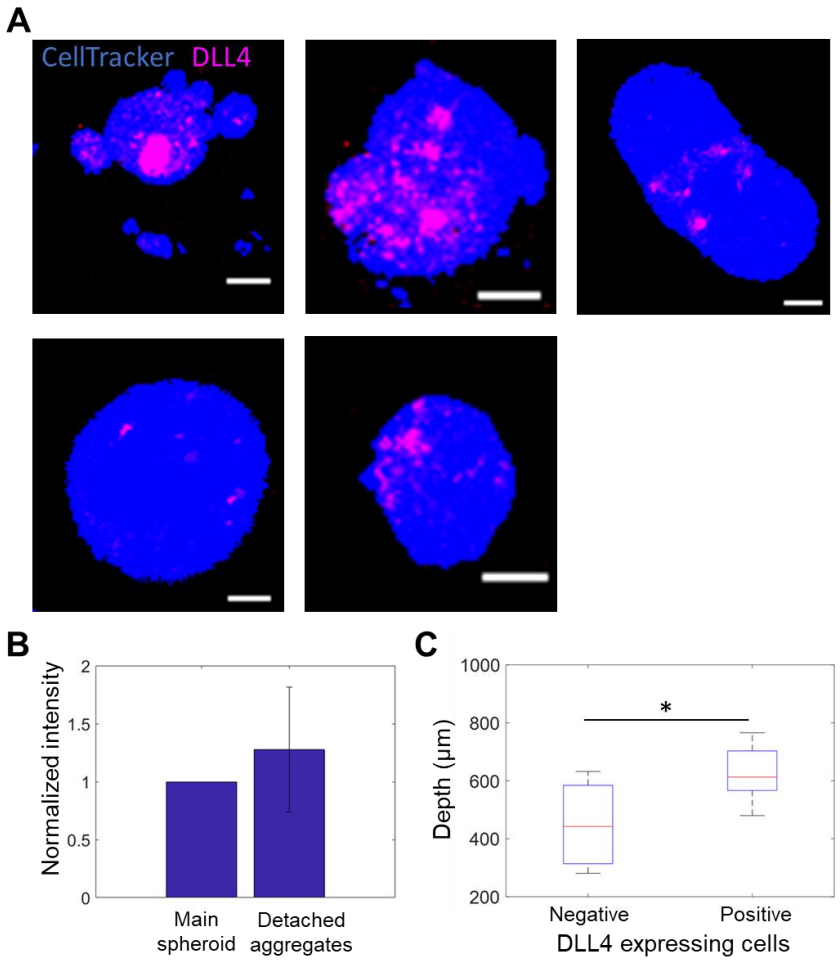

Figure 13. Invasive cell aggregates detached from primary cell spheroid (A) Cross section views of representative detached cell aggregates (blue) with GNR-LNA biosensor for DLL4 mRNA (red). The cells were obtained from a high-grade papillary urothelial carcinoma sample. Scale bar, 20μm. (B) Comparison of the Dll4 expression in the boundary of the main spheroids and detached aggregates. (C) Invasion depth of cell aggregates with and without DLL4 expression. (Negative n = 4; Positive n = 13; *p < 0.05; two-tailed unpaired Student's t-test). Source: Torab, P. et al. Three-Dimensional Microtumors for Probing Heterogeneity of Invasive Bladder Cancer. Anal. Chem. 92, 8768–8775 (2020).

3.2 Discussion

In this chapter, a simplified 3D microtumor assay was demonstrated for assessing the phenotypic heterogeneity of bladder cancer cell invasion at multiple levels. First, the model is designed to analyze the capability of cancer cells to degrade and penetrate the type of extracellular matrix found in the basal lamina. Interactions with healthy urothelial cells, fibroblasts, and other

basement membrane components that could affect invasion are not considered. Furthermore, the basement membrane is typically less than 100 nm thick, so significant invasion in our model does not necessarily imply that these cells would invade the same distance when crossing the basement membrane and invading the lamina propria *in vivo*. Rather, cells that have a high potential to penetrate the simulated basement membrane ECM in our model are expected to be more likely to cross the basement membrane *in vivo*, which represents a crucial first step in bladder cancer invasion.

The applicability of this invasion assay for characterizing the invasive subtypes within cellular populations is supported by the use of several established bladder cancer cell lines. While all cell lines exhibited considerable mobility on the ECM substrate and self-assembled into microtumor structures, some cell lines, including the basal subtype HT-1376 and invasive non-type UM-UC-3 lines, exhibited more aggressive behavior in regards to invading the ECM compared to luminal cells. The data are in good agreement with previous ex vivo and in vivo studies,[46,48,49] supporting the use of the model for characterizing the invasiveness of bladder cancer. The results indicate that microtumor invasiveness is a distinct feature compared to cell mobility on a 2D substrate, underscoring the importance of 3D invasion assays in studying bladder cancer invasiveness.

Second, the microtumor invasion assay captured the molecular heterogeneity within an individual cell line, thus identifying subpopulations with enhanced invasive capabilities. Unlike conventional techniques, such as the hanging drop method, self-assembly of bladder cancer cells on ECM can create hundreds of microtumors in each well simultaneously, allowing the molecular diversity of subpopulations to manifest. Compared with other tumor organoid models,[22–24] the on-gel microtumor self-assembly approach is amendable with GNR-LNA biosensors for single cell analysis and genetic modification.

Third, the coordination within the invasive microtumors was investigated, and the formation of invasive leader cells in invading microtumors was observed. In traditional 2D migration assays, such as the monolayer wound healing assay, emerging evidence supports a "leader" cell phenotype that positions at the leading edge, and it has been previously demonstrated that DLL4 mRNA is a molecular signature of leader cells.[20] Invasive leader cells with basal features were reported in

breast cancer invasion; however, the leader-follower organization remains poorly understood in the invasion of other cancer types.[27,31] By incorporating a GNR-LNA biosensor, DLL4 upregulation in the leading front of microtumors was revealed, and a positive correlation between DLL4 expression and invasion depth was observed. These results provide evidence in the involvement of invasive leader cells in the organization of bladder cancer invasion.

These results suggest NOTCH1-DLL4 signaling regulates the invasion of bladder cancer. DLL4, which is a ligand for NOTCH1 receptor, plays an important role in angiogenesis and wound healing.[20,51,56,57] Previous studies have noted a correlation between DLL4 expression and progression of several cancer types.[62,63] The mechanistic basis of anti-DLL4 therapy, however, is only partially understood, and multiple mechanisms have been proposed for anti-DLL4 therapy.[64] For instance, DLL4 is a target of therapy based on anti-tumor angiogenesis and is associated with proliferation and differentiation of cancer stem cells.[65] In the experiments described in this chapter, DLL4 was upregulated in invasive microtumors formed by cell lines and patient derived cancer cells. A correlation was observed between DLL4 expression and the invasion depth of the microtumor. Our results also indicated that NOTCH1 negatively regulates DLL4 during microtumor invasion. NOTCH1 inhibition by DAPT or siRNA enhanced the expression of DLL4 and the invasiveness of the microtumors. In contrast, transient knockdown of DLL4 resulted in a reduction of DLL4 expressing cells and the invasiveness of the microtumors (Figure 11). These results collectively suggest DLL4 inhibition may contribute to the anti-cancer effect by attenuating the invasive subpopulation and invasive leader cells. In the future, investigation should be performed to elucidate the mechanistic function of DLL4 in tumor invasion. Clinical studies will be required to decipher the role of DLL4 in the formation of invasive leader cells and evaluate the potential of anti-invasion therapy by targeting DLL4.

Pathologic interpretation of tissue specimens has been the major approach for bladder cancer staging and classification for over a century. Since it is difficult to predict the clinical outcome of bladder cancer patients, the 3D invasion assay may serve as a phenotypic surrogate assay for characterizing the invasiveness of patient tumor samples. Experimental results show that the 3D invasion assay and the GNR-LNA biosensor are compatible with primary cancer cells obtained from TURBT.

In the future, the inclusion of additional simulated tissue layers and incorporation of stromal cells will be required to better evaluate the interactions between the tumor and the microenvironment. The incorporation of a second layer mimicking the lamina propria is discussed in detail in Chapter 4. The protocol for isolating patient-derived tumor cells should also be further optimized to improve the efficiency and capture other stromal cells. Furthermore, molecular subtyping with high-throughput sequencing techniques and bioinformatics will provide useful information for guiding the treatment of muscle invasive bladder cancer.[8–10] The collection of these technologies will potentially enable a comprehensive approach for guiding personalized treatment of bladder cancer in the future.

3.3 Conclusion

This chapter demonstrated a 3D microtumor approach along with a single cell biosensor that overcomes some limitations of existing cancer models by targeting the invasive subpopulation. The microtumor approach was demonstrated with established cell lines and human clinical specimens derived from TURBT. This strategy can be applied to investigate cancer invasion mechanisms and to potentially guide treatment options for bladder cancer patients. A preliminary investigation of NOTCH1-DLL4 signaling in microtumors revealed that NOTCH1 suppression enhances DLL4 expression. Initial results suggest that enhancing DLL4 expression, via γ-secretase inhibition or NOTCH1 suppression, increases the invasion depth of microtumors. Conversely, DLL4 suppression appears to reduce the invasion depth. Collectively, these results indicate that the NOTCH1-DLL4 signaling pathway is involved in tumor progression in bladder cancer.

Chapter 4

Studying Interaction of Bladder Cancer Cell Subpopulations

4.1 Results

4.1.1 Presence of Two Subtypes Enhances Invasion in Simplified Model

The presence of multiple histologic variants within a bladder cancer tumor is common, and molecular heterogeneity is often observed when multiple variants are present.[5,11] The effects of intratumoral heterogeneity on bladder cancer progression and treatment response remain poorly understood.[7] To study these effects, the cellular subtypes described in section 1.1.2 were combined to form co-culture microtumors. Using the simplified model described in Chapter 3, 2 cell lines representing the luminal subtype (UM-UC-1, RT4) and 4 cell lines representing the basal subtype (SCaBER, HT-1197, HT-1376, 5637/HTB9) were tested individually and in every possible basal-luminal combination using the methodology described in Section 2.2.1. For co-culture experiments, cell lines were stained separately with CellTracker Green CMFDA and CellTracker Red CMTPX, then mixed 1:1. As with individual cell line experiments, a total of 10^4 cells was applied to each well.

Out of 8 total combinations, there was a significant increase in the median invasion depth during co-culture compared to the basal cell line in 6 cases (75%), and there was a significant increase in the median invasion depth compared to the luminal cell line in 7 cases (88) (one-tailed Wilcoxon rank sum test, see Table 2). The invasion depth results are given in Figure 14 and Figure 15. The combination of SCaBER (basal) and UM-UC-1 (luminal) cells was selected as a representative condition for subsequent experiments, as there was a significant in invasion depth observed between the individual cell lines and also between each individual cell line and the co-culture case (Figure 14, Supplementary Figure S7).

Luminal Cell Line	Basal Cell Line	Luminal Median < CC	Basal Median < CC
UM-UC-1	SCaBER	***	***
UM-UC-1	HT-1197	***	***
UM-UC-1	HT-1376	***	ns
UM-UC-1	5637	**	*
RT4	SCaBER	***	***
RT4	HT-1197	***	**
RT4	HT-1376	***	ns
RT4	5637	ns	***

Table 2. Basal luminal combinations increase invasion depth. Results of comparison between individual cell line and co-culture invasion depth distributions. (*p<0.05, **p<0.01, ***p<0.001, one-tailed Wilcoxon rank-sum test).

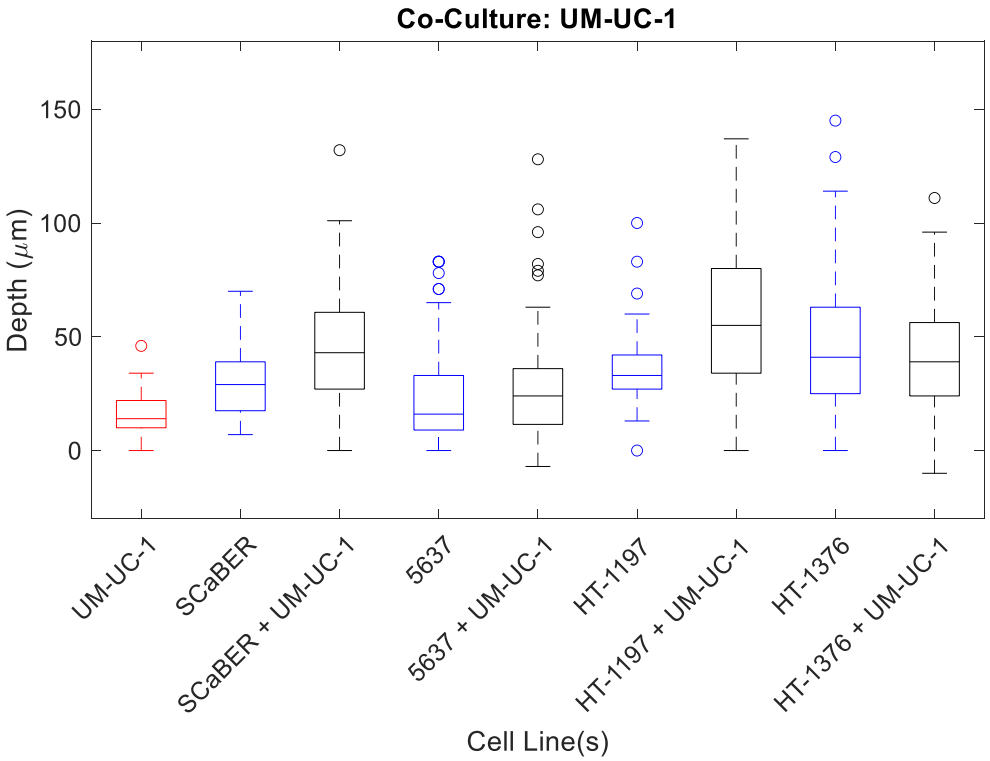

Figure 14. Co-culture with UM-UC-1. Depth distributions of luminal type cell line UM-UC-1 (red) and four basal cell lines (blue), along with 1:1 co-culture of basal and luminal cell lines (black). Obtained using simplified model.

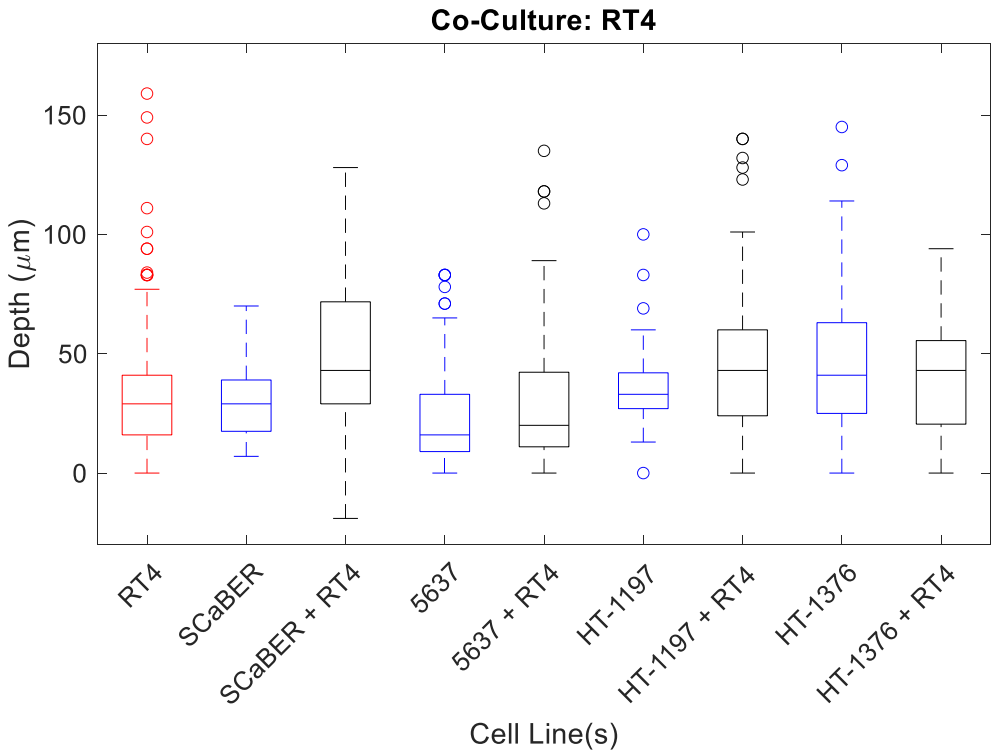

Figure 15. Co-culture with RT4. Depth distributions of luminal type cell line RT4 (red) and four basal cell lines (blue), along with 1:1 co-culture of basal and luminal cell lines (black). Obtained using simplified model.

4.1.2 SCaBER and UM-UC-1 Co-Culture Enhances Invasion in Multilayer Model

To further investigate the effect of heterotypic cellular interaction on microtumor invasion, SCaBER and UM-UC-1 cells were tested individually and in co-culture within the full, multilayer model using the protocol described in Section 2.2.3, representing the basal lamina and lamina propria. In addition to vertical invasion depth, the full model characterizes microtumors' ability to breach the basal lamina and invade the type of ECM found in the underlying lamina propria. The ability of a tumor to progress through both of these layers would indicate that the tumor has the potential to progress to MIBC, while less aggressive tumors would not be expected to progress through the simulated basal lamina layer. Furthermore, the number of microtumors that progress to a certain layer can simply be counted, as shown in Figure 16, eliminating the need for depth measurements, which can be difficult to interpret in the multilayer model as some variation in layer thickness occurs during assembly. The progression results for the individual cell lines and co-culture are given in Figure 17. SCaBER microtumors were found to be more invasive than UM-

UC-1, and co-culture microtumors were much more invasive than those generated from either individual cell line. This trend is in agreement with preliminary experiments carried out using the simplified model. The multilayer model, however, captures the ability of microtumors to penetrate both types of ECM found in the bladder wall between the urothelium and the first smooth muscle layer.

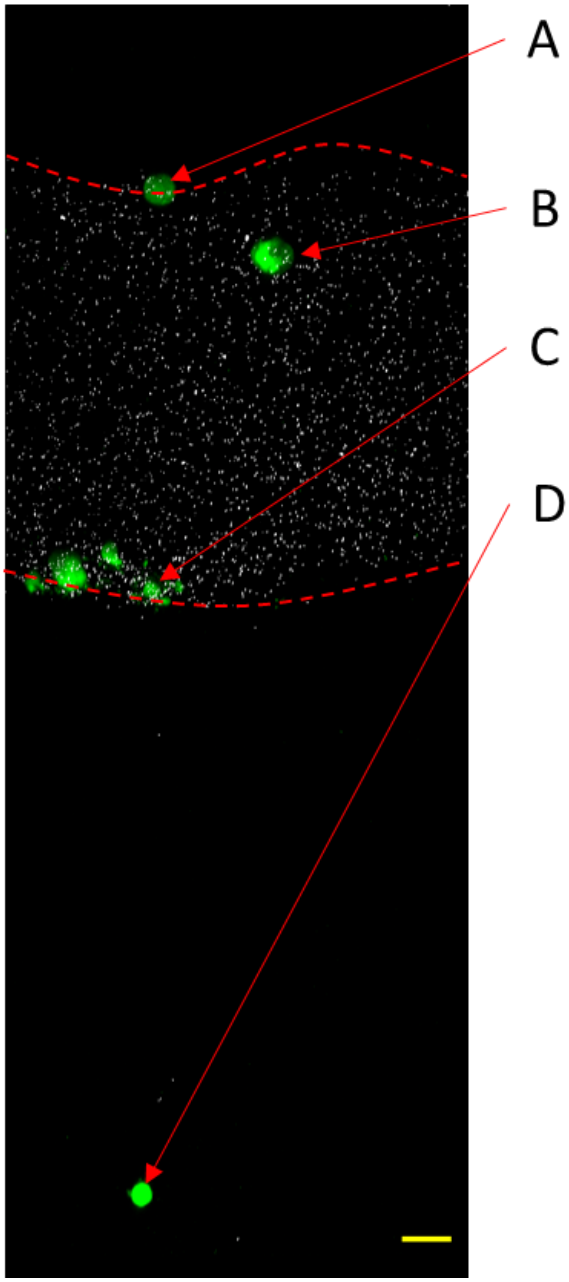

Figure 16. Classification Scheme for Full Multilayer Model. Representative image showing region-based classification of microtumor. The color scheme shown below is used in the following figures to indicate the regions in which microtumors were observed.

The microtumors (green) are shown interacting with the full multilayer model. The basal lamina layer is labeled with fluorescent beads (white). The region above this layer contains serum-free culture medium, and the region below this layer contains the simulated lamina propria.

Microtumors at the basal lamina interface (A, ■) remain on top of the gel after formation and do not invade. Microtumors embedded in the Matrigel (B, ■) are unable to reach the lamina propria after 72 hours. Microtumors at the basal lamina-lamina propria interface (C, ■) reach but do not invade the lamina propria. Finally, microtumors that progress through all layers are embedded in the lamina propria (D, ■)

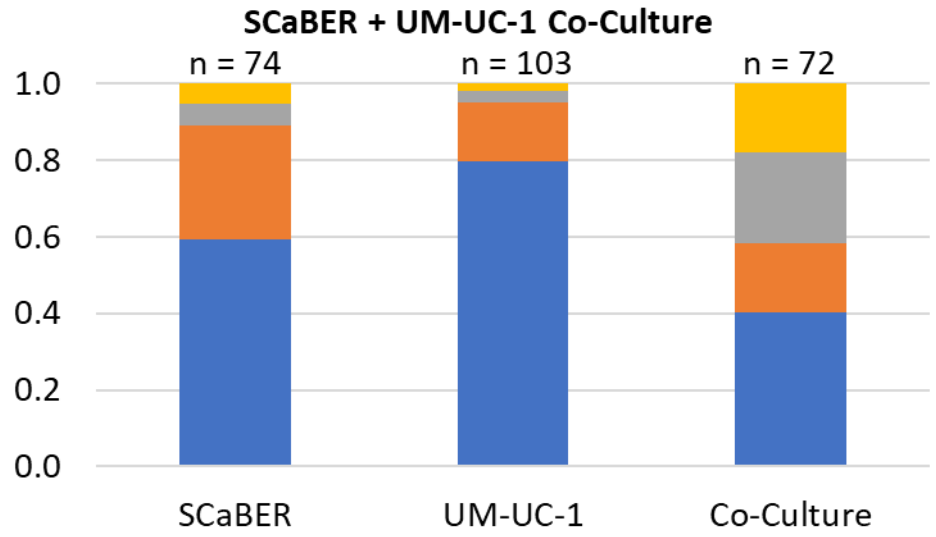

Figure 17. Distribution of invading microtumors in multilayer model. Fraction of microtumors observed on top of the basal lamina (blue), embedded in the basal lamina (orange), at the basal lamina – lamina propria interface (gray), and embedded in the lamina propria (yellow) 72 hours after seeding cells in the full multilayer model.

4.1.3 NOTCH1-DLL4 Signaling in Microtumors Containing Multiple Cellular Subtypes

The effects of NOTCH1-DLL4 signaling on microtumor progression was investigated using the full multilayer model described in Section 2.2.3 and SCaBER/UM-UC-1 co-culture. GNR-LNA biosensors with sequences targeting NOTCH1 and DLL4 mRNA were applied in separate experiments to both SCaBER and UM-UC-1 cells, which were then seeded into the full model and imaged after 72 hours to measure target mRNA expression. The results are shown in Figure 18, and representative images are shown in Figure 19 (NOTCH1), and Figure 20 (DLL4). In co-culture, NOTCH1 expression reached an intermediate value between the expression values for individual cell lines. Interestingly, DLL4 expression in co-culture was higher than in either individual cell line. This implies that the presence of multiple subtypes may contribute to elevated DLL4 expression, which in turn increases microtumor invasiveness.

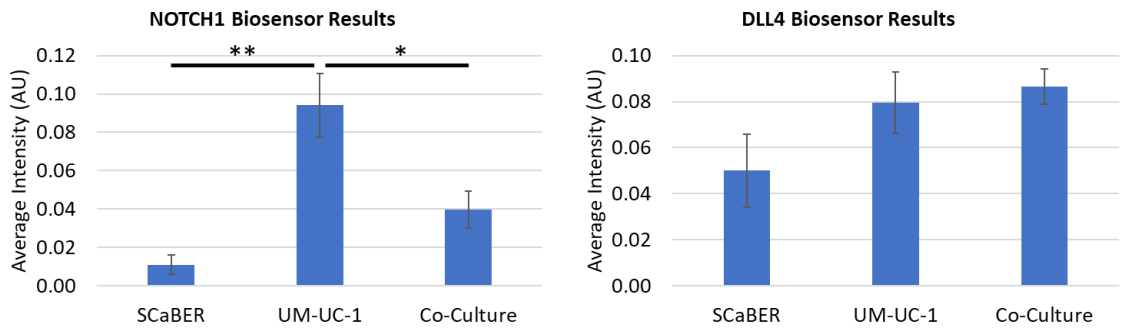

Figure 18. Average Expression of NOTCH1 and DLL4 in SCaBER, UM-UC-1, and co-culture. Average probe intensity (mean gray value) as a fraction of cell stain channel for a 3D image stack, which can be interpreted as volume average expression for all microtumors within field of view (arbitrary units) with standard error. Measured using NIH ImageJ. *p<0.05, **p<0.01 (1-way ANOVA with Tukey-Kramer post test)

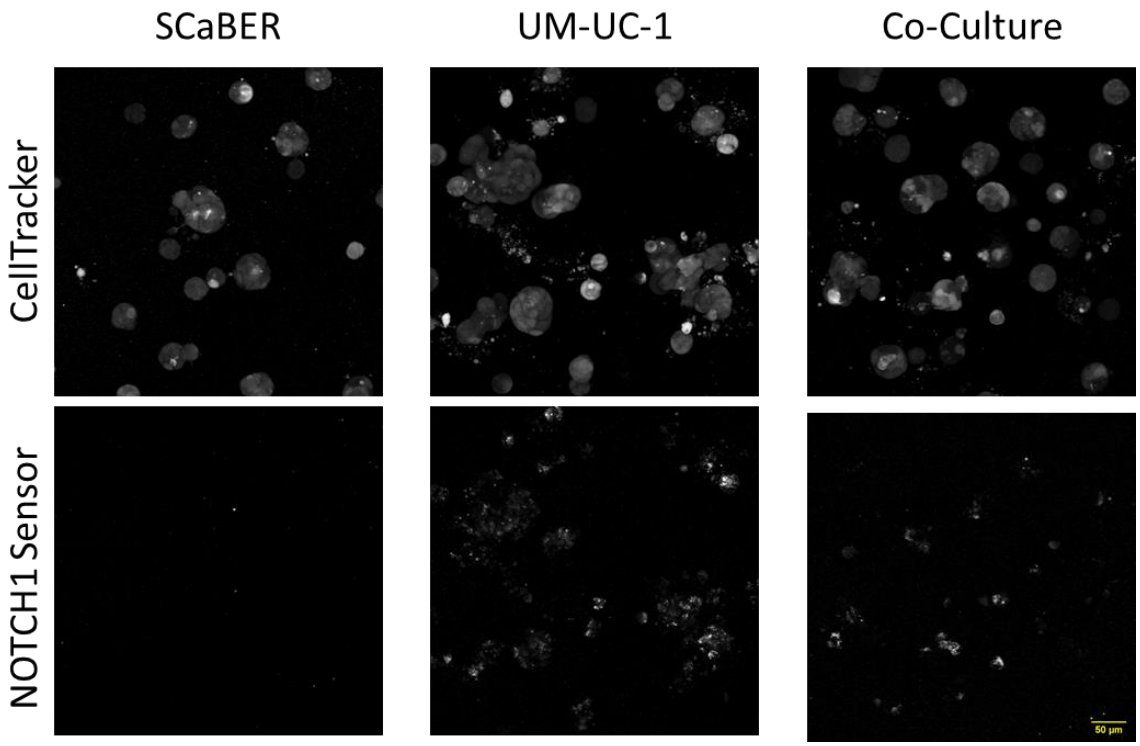

Figure 19. Expression of NOTCH1 in SCaBER, UM-UC-1, and co-culture. Representative images showing cell stain and NOTCH1 sensor signal in SCaBER, UM-UC-1, and co-culture. Scale bar: 50µm

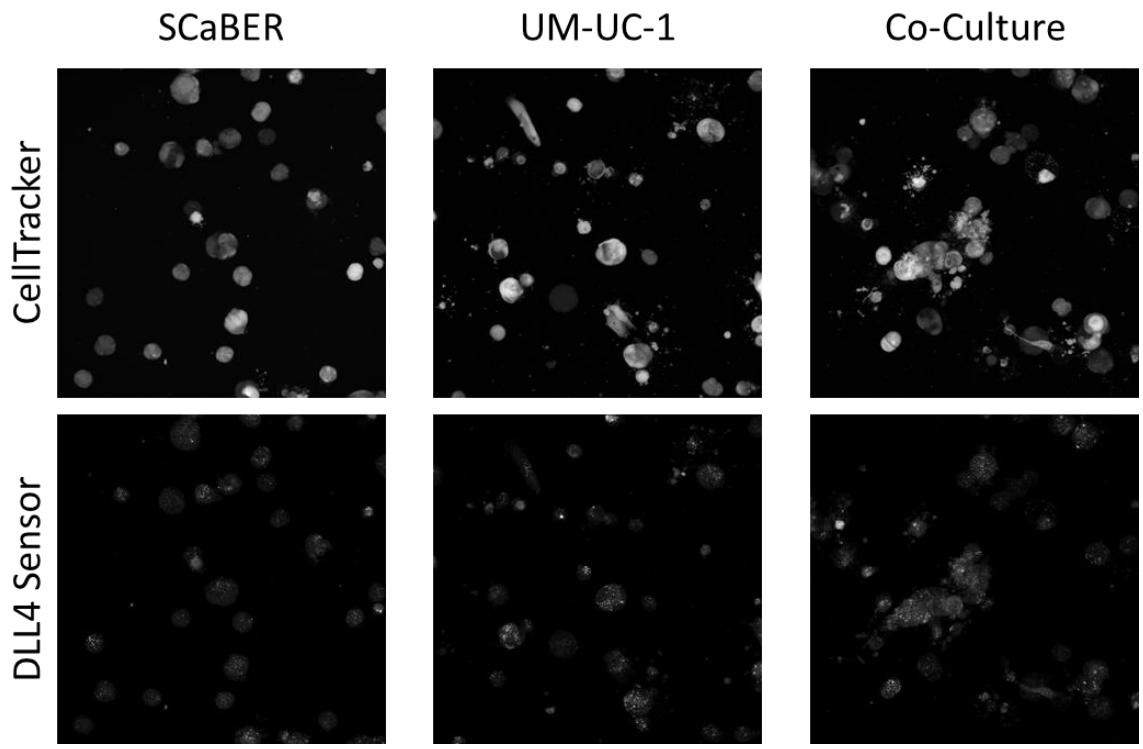

Figure 20. Expression of DLL4 in SCaBER, UM-UC-1, and co-culture. Representative images showing cell stain and DLL4 sensor signal in SCaBER, UM-UC-1, and co-culture. Scale bar: 50μm

4.1.4 DLL4 Inhibition Modulates Invasiveness of Co-Culture Microtumors

Inhibition of DLL4 signaling has been proposed as an anticancer therapy.[63–65] To test the effects of DLL4 inhibition on heterogeneous microtumors, SCaBER/UM-UC-1 co-culture spheroids with DLL4 transient knockdown were tested using the full model. SCaBER and UM-UC-1 were alternately treated with DLL4 siRNA and non-targeting (control) siRNA following the procedure described in section 2.2.3. Co-culture spheroids were formed using one cell line treated with DLL4 siRNA and another treated with non-targeting siRNA. Spheroids in which both cell lines were treated with DLL4 siRNA were also tested. Compared to co-culture without DLL4 knockdown (Figure 17), invasion was inhibited in all cases. More cells were observed at the medium interface and no cells reached the collagen layer, as shown in Figure 21. Although the wild type cell lines exhibited differences in DLL4 expression, interestingly, DLL4 knockdown reduced invasion when applied to either cell line or both cell lines with similar efficiency.

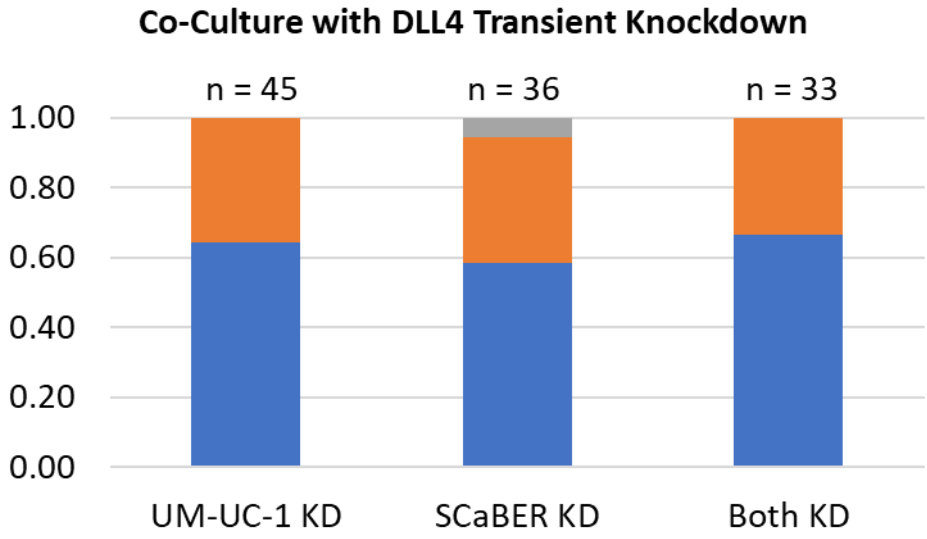

Figure 21. Distribution of invading microtumors with DLL4 transient knockdown. Fraction of microtumors observed on top of the basal lamina (blue), embedded in the basal lamina (orange), at the basal lamina – lamina propria interface (gray), and embedded in the lamina propria (yellow) 72 hours after seeding cells in the full multilayer model. All three cases represent SCaBER/UM-UC-1 co culture. The cell line labeled KD is treated with DLL4 siRNA and the other is treated with non-targeting siRNA.

4.1.4 NOTCH1 Inhibition Enhances Invasion of Co-Culture Microtumors

NOTCH1 is believed to function as a tumor suppressor in bladder cancer, and disruptions in NOTCH signaling have been found to promote tumor progression in bladder cancer.[14,17] To test the effect on NOTCH1 inhibition, SCaBER/UM-UC-1 co-culture microtumors with NOTCH1 transient knockdown applied to one cell line were tested using the full model. The cell line not treated with NOTCH1 siRNA was treated with non-targeting siRNA. In both cases, NOTCH1 inhibition produced an increase in invasiveness compared to co-culture without transient knockdown (Figure 17), as shown in Figure 22. Unlike other conditions that produced a high likelihood of invasion, no cells were detected at the basal lamina-lamina propria interface, suggesting that NOTCH1 activity may be related to cellular mechanisms for invading collagen 1 specifically. This will be discussed further in Chapter 5.

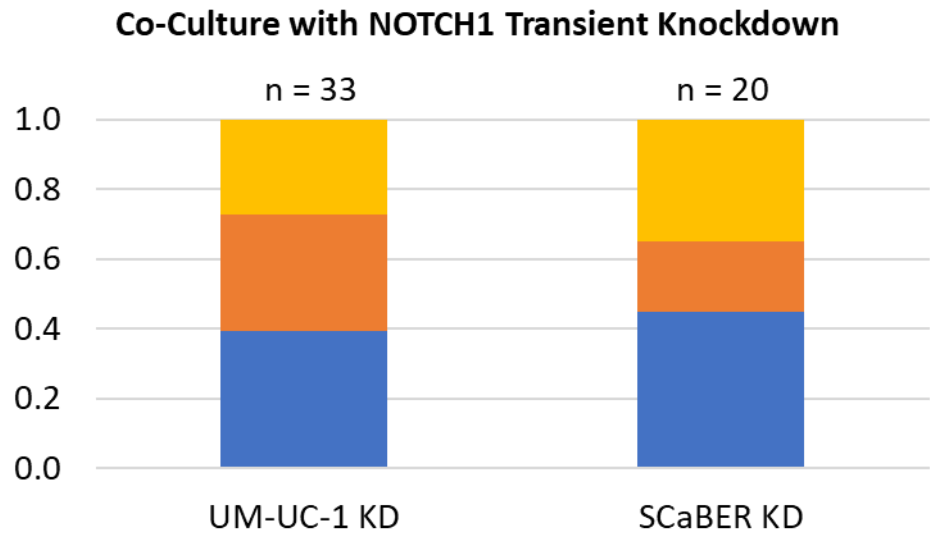

Figure 22. Distribution of invading microtumors with NOTCH1 transient knockdown. Fraction of microtumors observed on top of the basal lamina (blue), embedded in the basal lamina (orange), at the basal lamina – lamina propria interface (gray), and embedded in the lamina propria (yellow) 72 hours after seeding cells in the full multilayer model. All three cases represent SCaBER/UM-UC-1 co culture. The cell line labeled KD is treated with NOTCH1 siRNA and the other is treated with non-targeting siRNA.

4.1.5 FOXA1 Knockout Enhances Invasiveness of UM-UC-1

Recent studies have indicated that FOXA1 is a marker of the luminal subtype, and that FOXA1 overexpression may drive basal bladder cancer cells to assume a more luminal phenotype.[45,66] As a result, altering FOXA1 expression has emerged as a possible strategy to induce the less aggressive luminal phenotype. To study the effect of FOXA1 expression on invasiveness, an invasion assay was performed on UM-UC-1 cells with CRISPR-Cas9 knockout of FOXA1 (Source) in the full model. UM-UC-1 FOXA1-KO cells were also co-cultured with wild type cells. The results are shown in Figure 23. UM-UC-1 cells with FOXA1 knockout were found to be slightly more likely to invade the basal lamina and much more likely to reach the lamina propria. Interestingly, co-culture spheroids were much more likely to invade and less likely to become trapped at the basal lamina-lamina propria interface. RNA sequencing of FOXA1-KO cells revealed downregulation of NOTCH1 (Supplementary Figure S9), indicating a possible connection between NOTCH1 and FOXA1 expression.

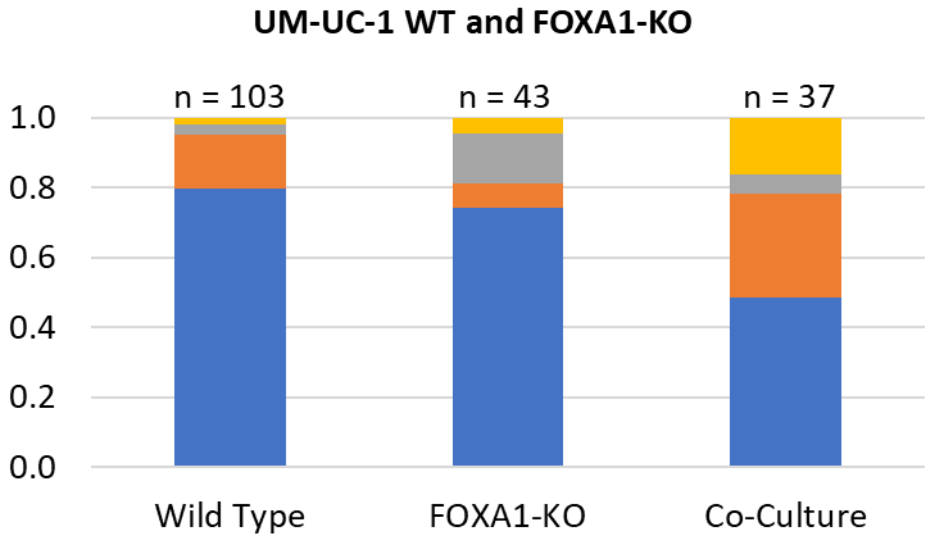

Figure 23. Distribution of UM-UC-1 microtumors with FOXA1 knockout. Fraction of microtumors observed on top of the basal lamina (blue), embedded in the basal lamina (orange), at the basal lamina – lamina propria interface (gray), and embedded in the lamina propria (yellow) 72 hours after seeding cells in the full multilayer model.

4.2 Discussion

In this chapter, a novel multilayer microtumor assay was used to characterize the effects of intratumoral heterogeneity on tumor progression through the bladder basal lamina and lamina propria. As with the simplified model, the effects of healthy urothelial cells, fibroblasts, and other components are not considered. This assay has the unique capability of screening cancer cells for their potential to breach the basal lamina and then subsequently invade the lamina propria. The ability to cross both layers suggests that a cell line or combination of cell lines has the potential to progress to MIBC, an important distinction in prognosis and management of bladder cancer. As with the simplified model, the invasive behavior observed is in good agreement with previous studies.[46,48,49]

The combination of SCaBER and UM-UC-1, representing basal and luminal cellular subtypes, respectively, was examined in detail. This combination was selected because of the significant difference in behavior between these two cell lines individually, and also due to the significant

enhancement of invasion observed in co-culture using the simplified model, as shown in Figure 14 and Supplementary Figure S7. Although this combination does represent heterotypic interaction between basal and luminal cells, further work is required to fully understand both the role and specific mechanisms of this interaction as they relate to tumor progression. In the full multilayer model, SCaBER and UM-UC-1 showed much higher invasive potential in co-culture than either cell line individually, as shown in Figure 17. Interestingly, a large number of cells were detected at the interface between the basal lamina and lamina propria layers, suggesting that the ability to breach the basal lamina alone is not sufficient to characterize the invasiveness of a bladder cancer tumor. Logical continuations of this work would include further development of the multilayer tissue model to include other important components, such as fibroblasts, healthy urothelial cells, and microvasculature (or nutrient supply) and simply the testing of more cell lines and combinations in the multilayer model. The behavior of primary cells derived from patient tumor samples is of particular interest.

The role of NOTCH1-DLL4 signaling was investigated in SCaBER and UM-UC-1 individually and in co-culture using a GNR-LNA biosensor. NOTCH1 was upregulated in UM-UC-1 when compared to SCaBER and co-culture. This piece of evidence lends support to the proposed role of NOTCH1 as a tumor suppressor in bladder cancer[14,17], as UM-UC-1 microtumors were also significantly less invasive than SCaBER or co-culture in invasion assays using the simplified and multilayer experimental models (Figure 14, Figure 17). Furthermore, transient knockdown of NOTCH1 via RNA interference enhanced invasion depth in HT-1376 in the simplified model (Figure 11), and increased progression to the lamina propria layer when applied to either cell line in SCaBER/UM-UC-1 co-culture using the full model (Figure 22). Future work will study the effect of NOTCH1 knockdown on both SCaBER and UM-UC-1 in co-culture.

The expression of DLL4 was also studied using a GNR-LNA biosensor. Interestingly, DLL4 mRNA expression was slightly higher in co-culture than in either cell line individually. This is in contrast to NOTCH1 biosensor results, in which the co-culture microtumors exhibited an intermediate NOTCH1 mRNA expression level between the two individual cell lines (Figure 18, Figure 19). Co-culture microtumors were also more invasive than those generated from either cell line individually (Figure 17). However, of the two individual cell lines, UM-UC-1 had higher

DLL4 mRNA expression but was significantly less invasive compared to SCaBER (Figure 18, Figure 20). Clearly, the conclusion that DLL4 expression is directly related to invasiveness cannot be reached from these results. However, results suggest that forcing an upregulation of DLL4 can enhance invasiveness, and that DLL4 inhibition can modulate invasiveness in the same manner.

Taken together, these results support the view of DLL4 and NOTCH1 as a possible therapeutic targets in cancer, including in bladder cancer specifically.[18,59,64] Future work should seek to elucidate the mechanism(s) for invasion of bladder wall ECM, and the specific relationship with NOTCH1-DLL4 signaling. The results presented here should serve as preliminary evidence of the role of NOTCH1-DLL4 signaling in bladder cancer. Another clear trend is the effect of cellular and molecular heterogeneity on tumor invasiveness. As discussed previously, the presence of multiple cellular subtypes itself frequently increases the likelihood of invasion (Figure 14, Figure 15, Figure 16, Supplementary Figure S7, Supplementary Figure S8). Furthermore, perturbing NOTCH1-DLL4 signaling in one of two cell lines in co-culture is enough to produce significant changes in invasion (Figure 21 Figure 22).

Recent work has indicated FOXA1 as a marker of the luminal cellular subtype, and also as a driver of the luminal phenotype.[8,45,66,67] The role of FOXA1 was studied briefly using the multilayer invasion assay. Luminal type UM-UC-1 cells with CRISPR knockout of FOXA1 were observed to be slightly more invasive than wild type cells. Most interestingly, co-culture of wild type and FOXA1 knockout cells resulted in a clear increase in invasiveness and very few cells observed at the layer interface (Figure 23). As with NOTCH1-DLL4 signaling, one can conclude that molecular heterogeneity in FOXA1 expression itself may produce downstream effects that enhance tumor invasion. Further work should attempt to replicate these results with other cell lines representing both cellular subtypes.

4.3 Conclusion

In this chapter, a novel multilayer invasion assay was used to study the effects of cellular and molecular heterogeneity in bladder cancer tumors. The interaction between basal and luminal cellular subtypes was characterized by probing NOTCH1-DLL4 signaling and FOXA1, a molecular driver of the luminal subtype. Co-culture microtumors containing cell lines representing basal and luminal subtypes were generally more invasive than those generated from either cell line alone. A detailed investigation of SCaBER (basal) and UM-UC-1 (luminal) cells in co-culture revealed that DLL4 expression in co-culture can be higher than in either individual cell line, whereas NOTCH1 expression reached an intermediate level. DLL4 suppression in either cell line was found to inhibit microtumor invasion. Similarly, NOTCH1 suppression in either cell line enhanced invasion. The relationship between basal-luminal interaction and NOTCH1-DLL4 signaling in bladder cancer was investigated using UM-UC-1 cells. UM-UC-1 cells with CRISPR-Cas9 knockout of FOXA1, a marker of the luminal subtype, were co-cultured with wild-type cells. Invasion depth results revealed behavior similar to luminal-basal co-culture, in which the induced basal subtype (FOXA1 knockout UM-UC-1) was slightly more invasive than the luminal subtype (wild type UM-UC-1), but co-culture was more invasive than either individual cell line. RNA sequencing revealed that UM-UC-1 cells with FOXA1 knockout had reduced NOTCH1 expression compared to wild-type cells.

Chapter 5

Discussion

5.1 Experimental Models for Studying Cancer

The development of a novel, multilayer experimental model of bladder cancer was discussed in this dissertation. The model was utilized an invasion assay to characterize bladder cancer cell lines, including primary tumor cells derived from patient tissue samples. Unlike current experimental models, the multilayer bladder cancer model uses simulated basal lamina as the scaffold for microtumor self-assembly, as well as a first barrier that must be crossed before a tumor reaches a simulated lamina propria. The objective of this strategy was to create an invasion assay that better mimics the bladder wall in order to encourage modes of invasion that are closer to what is observed *in vivo*. In the future, such an assay could serve as a surrogate assay for preliminary screening of bladder cancer tumors to improve disease prognosis and rapidly test personalized treatment strategies. Further development is need in several areas. First, improvements must be made in the manufacturing of the multilayer model. In particular, strategies for reliably generating a thinner basal lamina should be explored. The basal lamina, sometimes referred to as the basement membrane, is thought to serve as a barrier to invasion, and the unrealistic thickness of this layer in the multilayer model may downplay the invasiveness of some cells. Reducing its thickness is crucial to increasing the physiological relevance of the assay for bladder cancer and other cancers. Second, the protocol used to generate the full model should be adapted for use in a multi-well microfluidic device. The ability to screen many samples or treatments at once would greatly improve the practicality of the multilayer model for research and future clinical applications. Finally, the multilayer model should be expanded to include more components of the tumor microenvironment. While it would be nearly impossible to include all relevant aspects of the microenvironment, incorporating additional cell types and improving the nutrient supply system would be relatively straightforward and would improve the physiological relevance of the model.

5.2 NOTCH1-DLL4 Signaling in Bladder Cancer

The NOTCH1-DLL4 signaling pathway was studied using pharmacological perturbation and RNA interference to reveal its role in bladder cancer tumor invasion. Results suggest that NOTCH1-DLL4 signaling is involved in and may be even be a key regulator of bladder tumor progression. Other researchers have proposed this involvement, but it has not been replicated experimentally in bladder cancer before. A deeper understanding of the underlying mechanisms will be crucial to determine the proper use and limitations of this novel multilayer invasion assay. In particular, the specific mode of invasion and its connection to NOTCH1-DLL4 remain unclear. The results of this study do suggest that NOTCH1-DLL4 may have promise as a therapeutic target.

5.3 Intratumoral Heterogeneity

Another unique aspect of this work is the inclusion of intratumoral heterogeneity at the molecular and cellular levels. Histologic variants representing different cellular subtypes have been observed in several clinical studies, and more recently, multiple cellular subtypes and molecular variants have been observed within the same tumor. This is believed to play a role in tumor progression and treatment response, and the results presented in this dissertation broadly support this view. Future work should include a comprehensive characterization of other established bladder cancer cell lines representing basal, luminal, and other cellular subtypes to further explore the effects of intratumoral heterogeneity. This would also help determine which classification scheme is most useful in predicting treatment outcomes. Connecting certain cellular subtypes to bladder tumor behavior could vastly improve prognosis and disease management.

Appendix

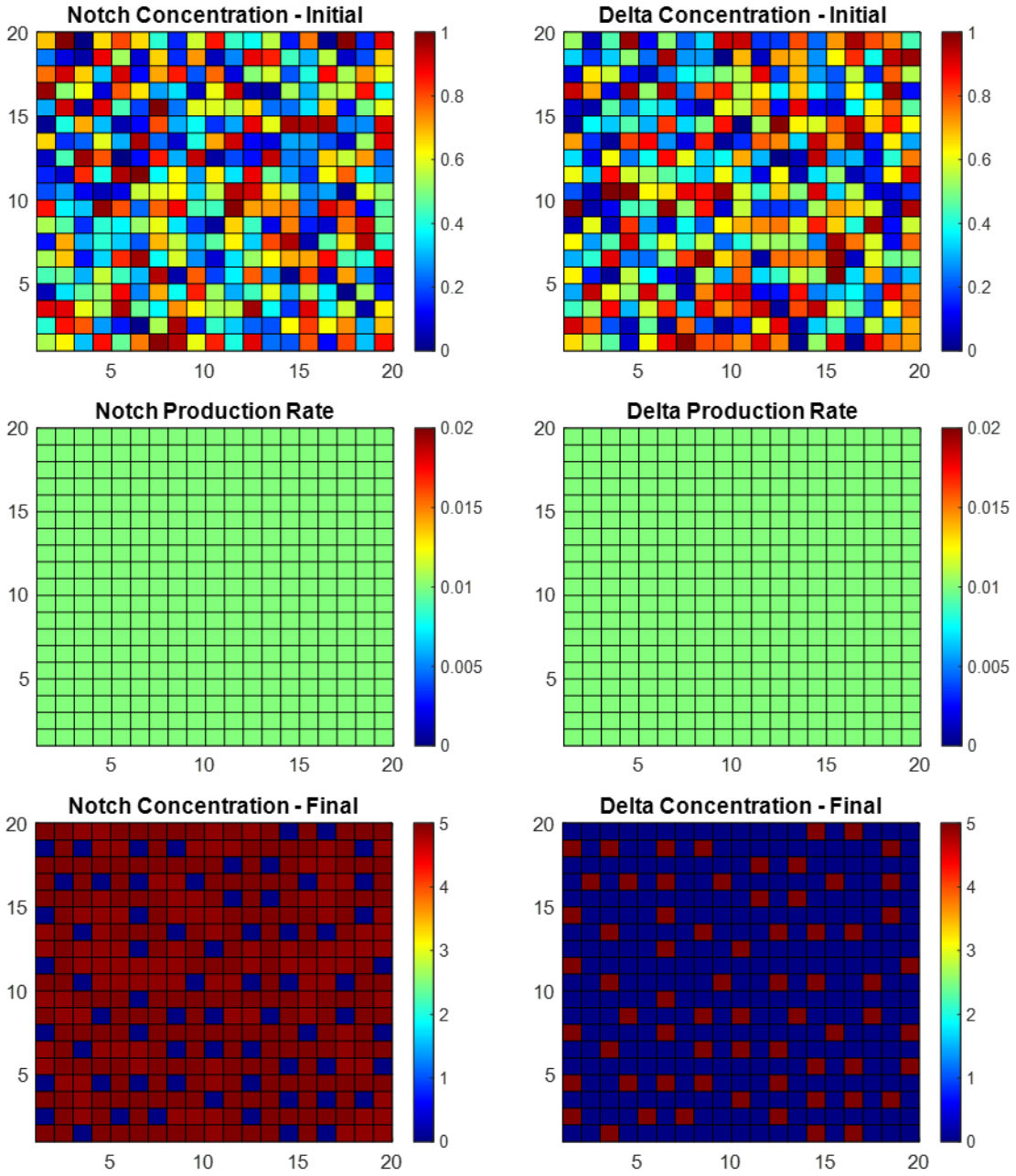

Figure S1. Numerical simulation of Notch-Delta signaling with uniform production rates. Uniform Notch and Delta production rates in all cells will result in pattern formation over time.

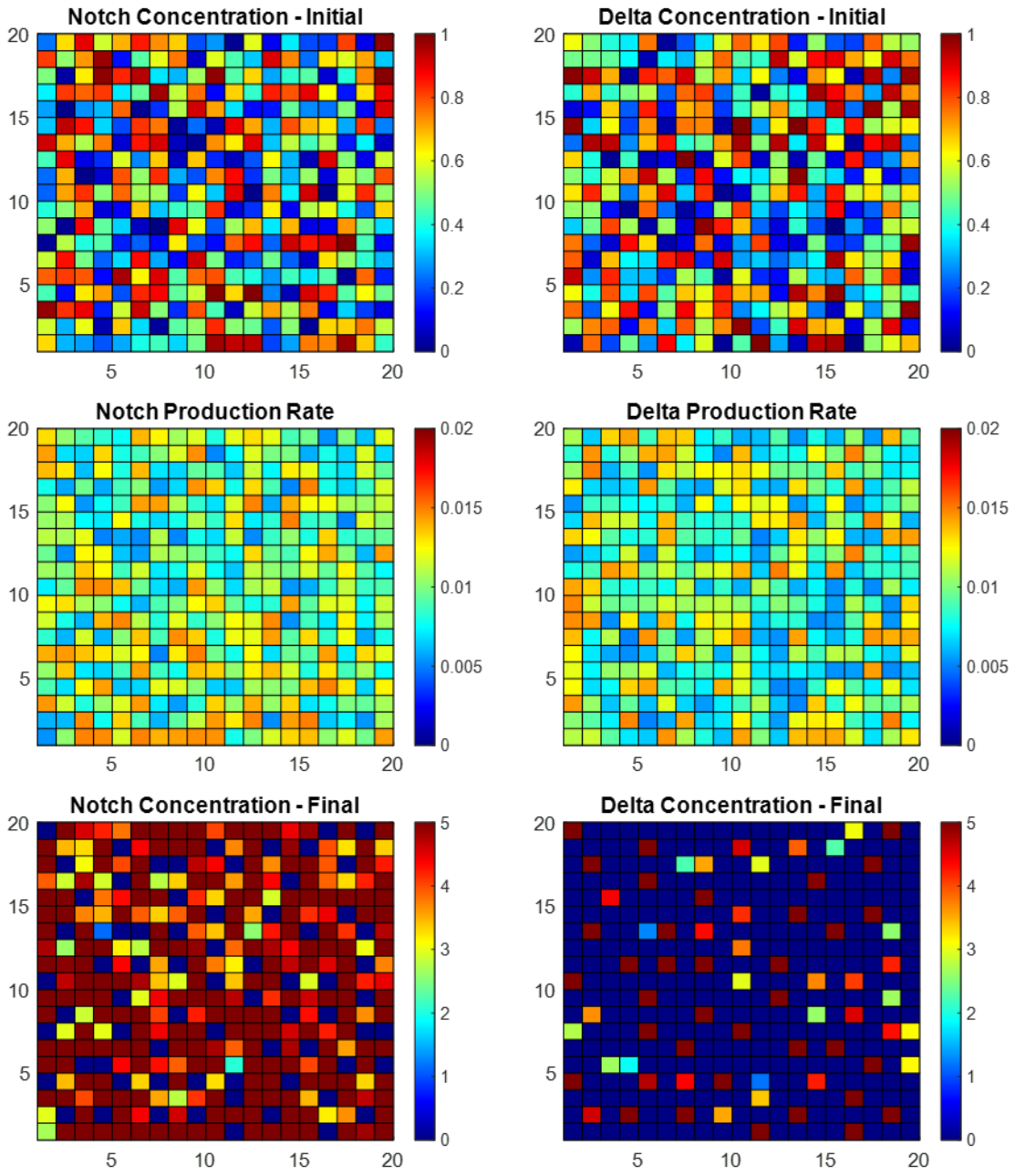

Figure S2. Numerical simulation of Notch-Delta signaling with non-uniform production rates. Randomly generated Notch and Delta production rates (±50% nominal value as shown) in all cells mimic variation expected in live cells.

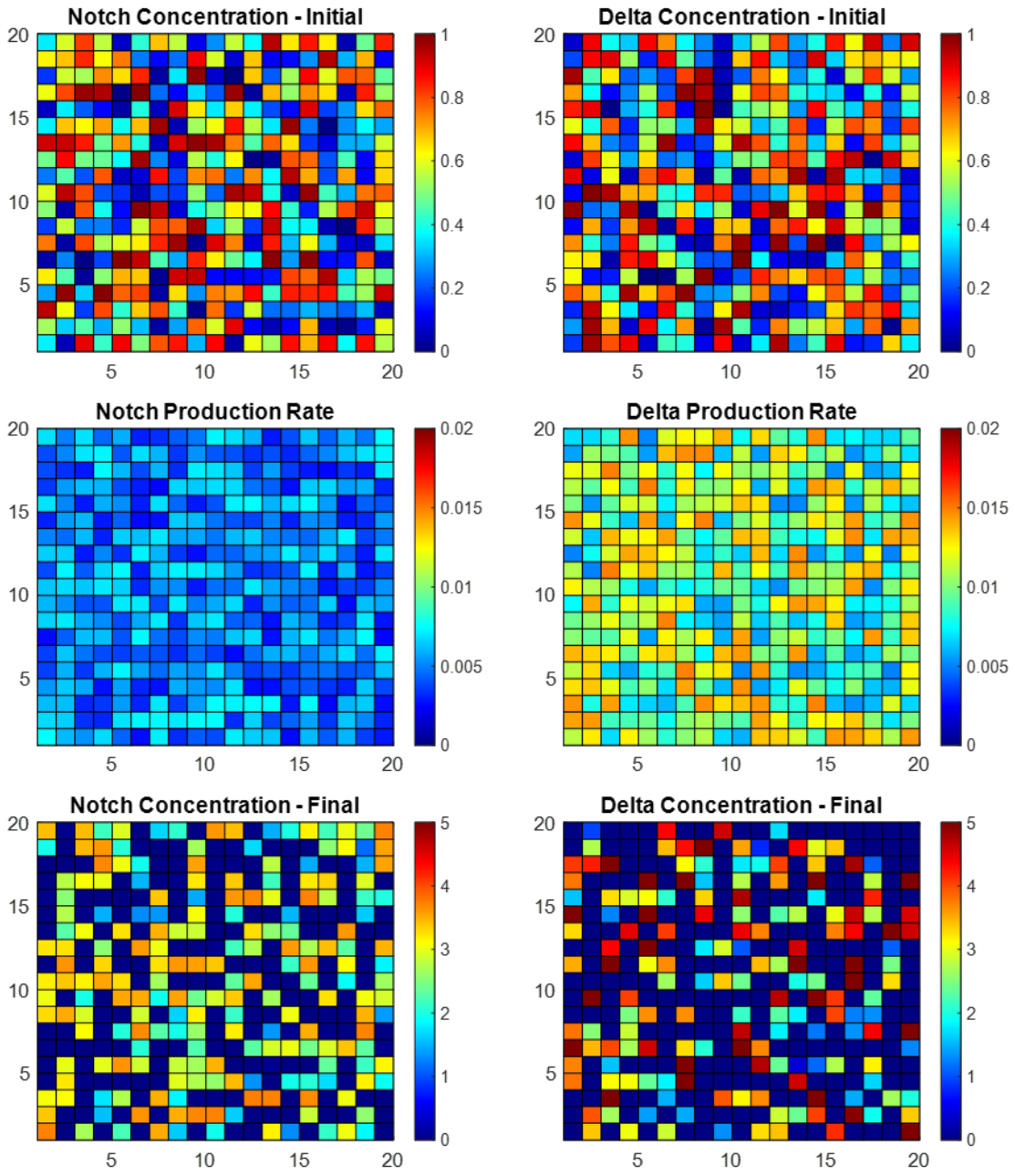

Figure S3. Numerical simulation of Notch-Delta signaling with Notch inhibition. A 50% reduction in nominal Notch production rate mimics Notch knockdown, resulting in a broad increase in DLL4 expression.

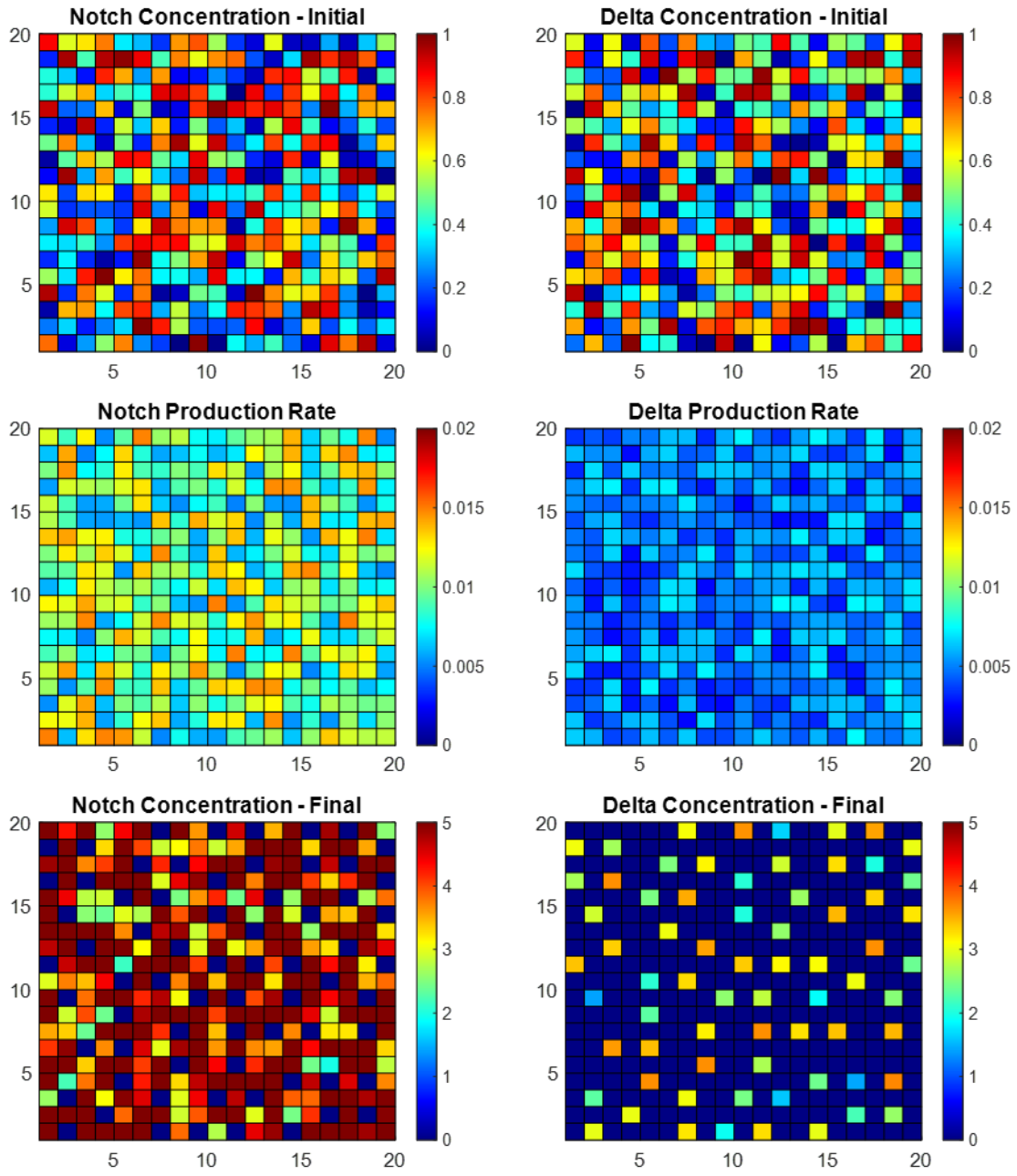

Figure S4. Numerical simulation of Notch-Delta signaling with Delta inhibition. A 50% reduction in nominal Delta production rate mimics Delta knockdown, resulting in decreased Notch and Delta expression.

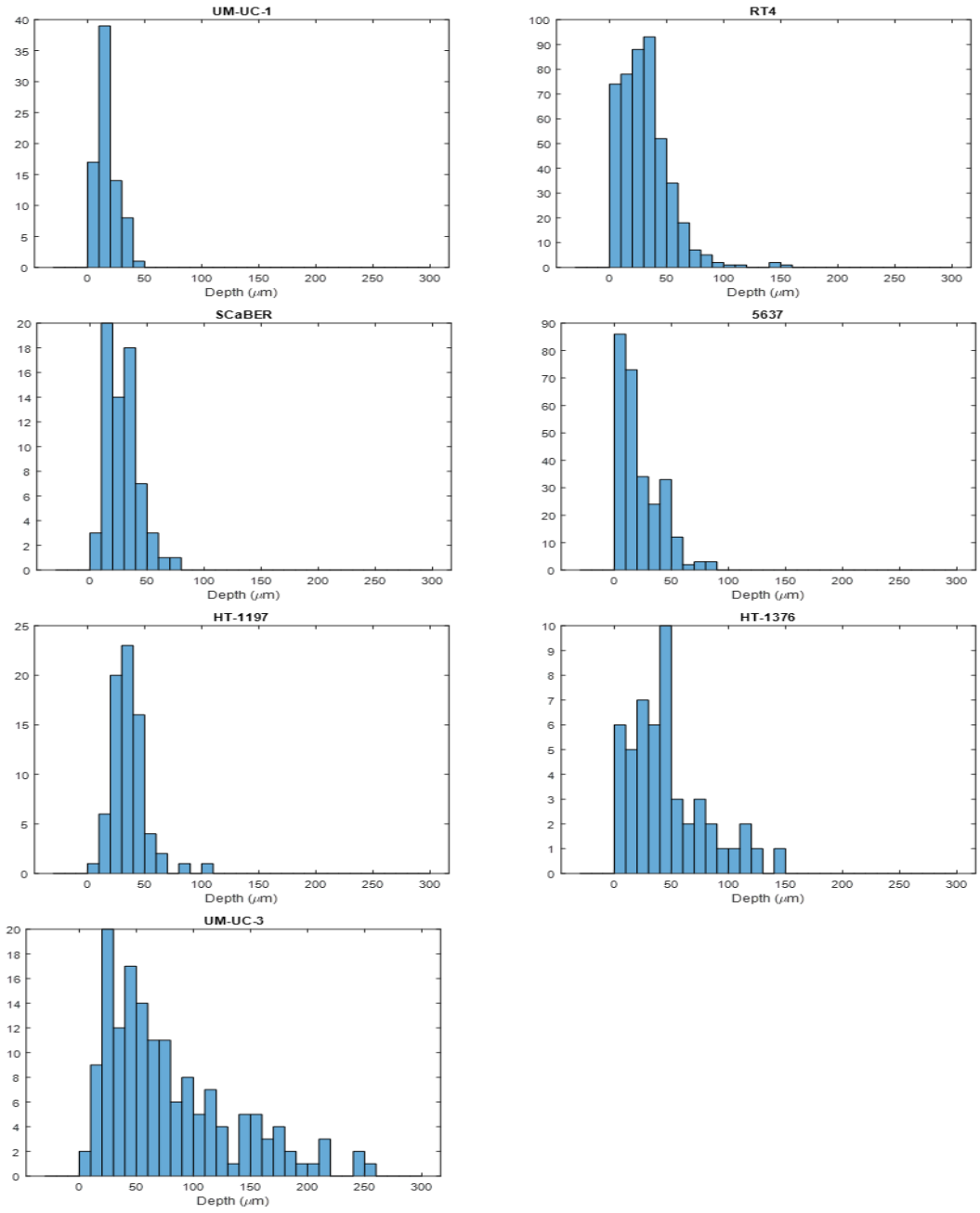

Figure S5. Depth distributions of individual cell lines. Histograms showing the invasion depth results for each individual cell line, tested using the simplified model.

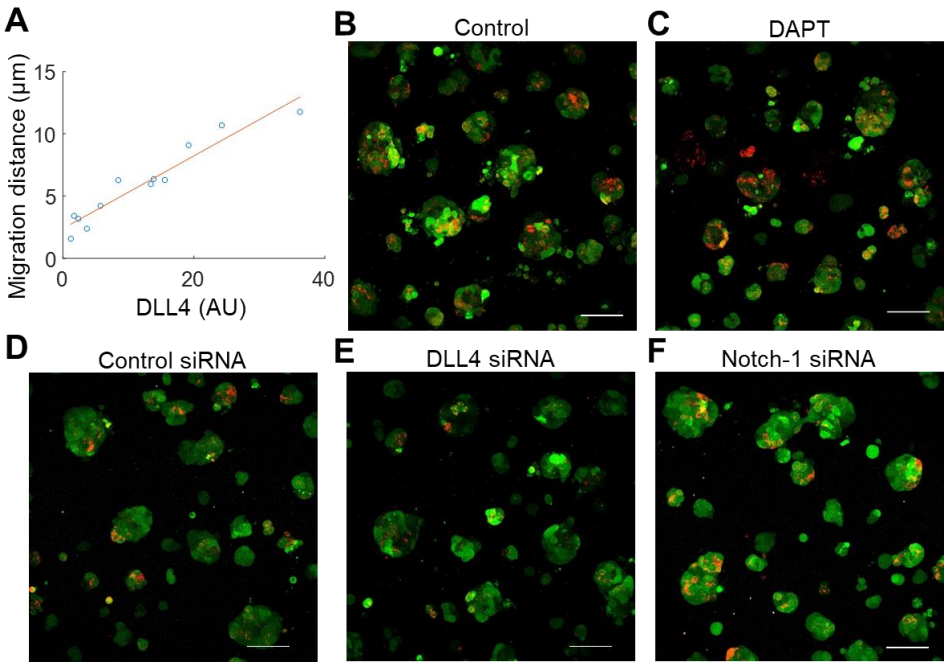

Figure S6. DLL4 expression is associated with the invasiveness of bladder microtumors. (A) The expression of DLL4 at the invading front is correlated with change in invasion depth over 72 hours. Red line represents regression analysis, which has an R-squared value of 0.9179. (B-F) Fluorescence images (vertical projection of 3D stack) for illustrating the effects of DAPT, DLL4 siRNA, and NOTCH1 siRNA on DLL4 expression. Images are representative of three independent experiments. Scale bar, 100 μm.

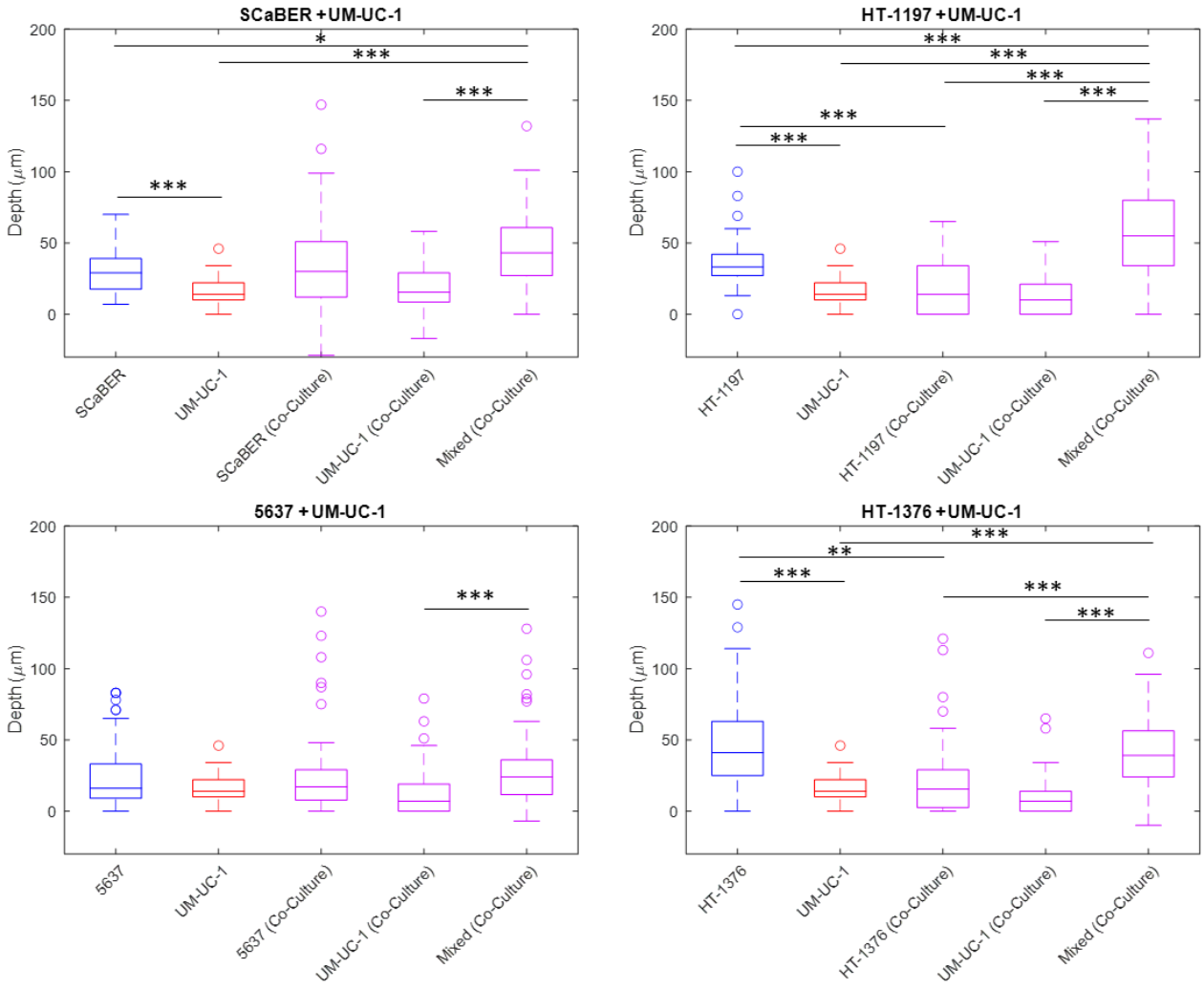

Figure S7. Detailed depth distributions for UM-UC-1 co-culture. Box plots showing the invasion depth distribution for each basal cell line (blue), UM-UC-1, (red), and co-culture (purple). Within co-culture results, the first box includes all-basal microtumors, the second includes all-luminal microtumors, and the third includes mixed microtumors that contained both cell lines.

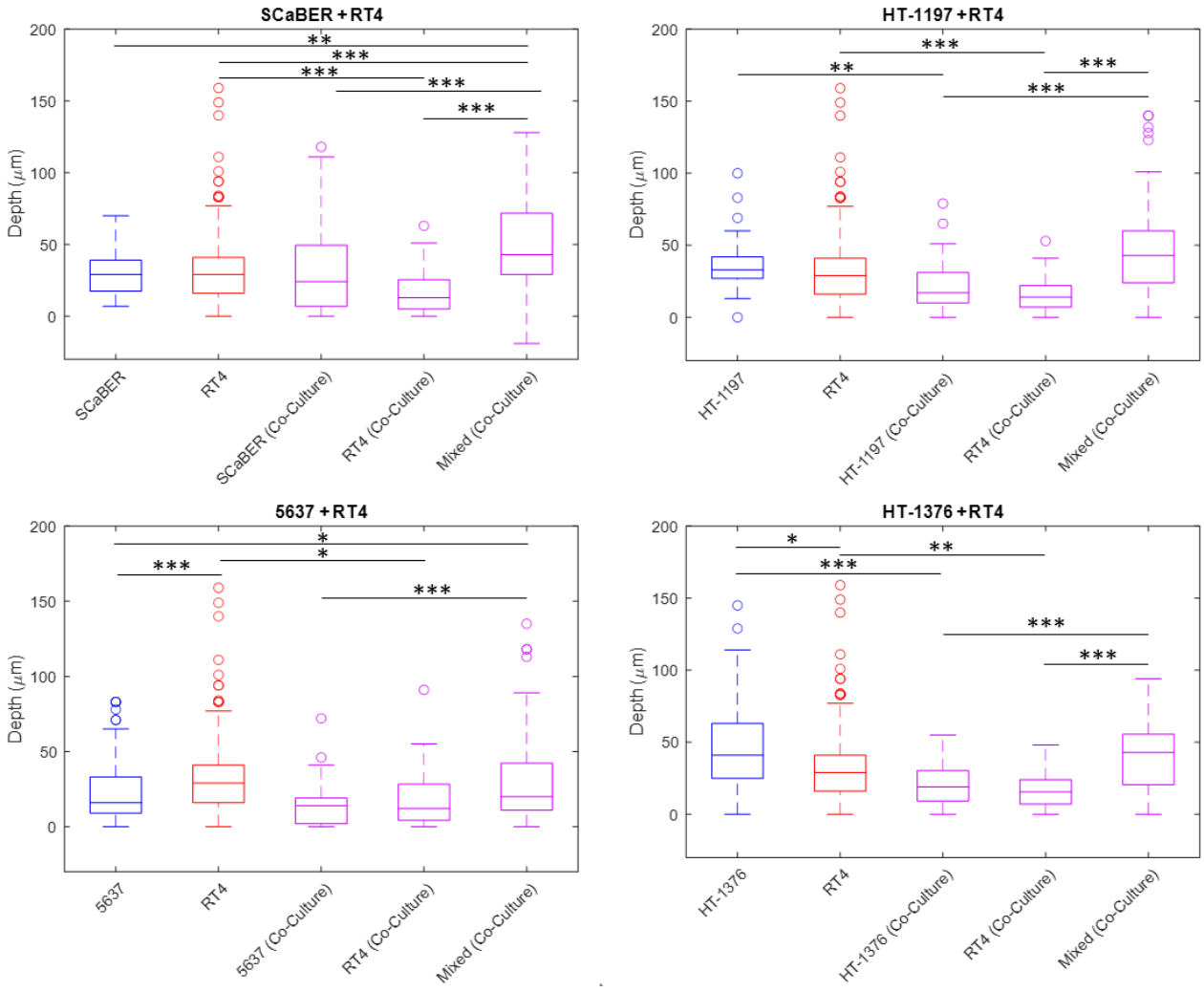

Figure S8. Detailed depth distributions for RT4 co-culture. Box plots showing the invasion depth distribution for each basal cell line (blue), RT4, (red), and co-culture (purple). Within co-culture results, the first box includes all-basal microtumors, the second includes all-luminal microtumors, and the third includes mixed microtumors that contained both cell lines.

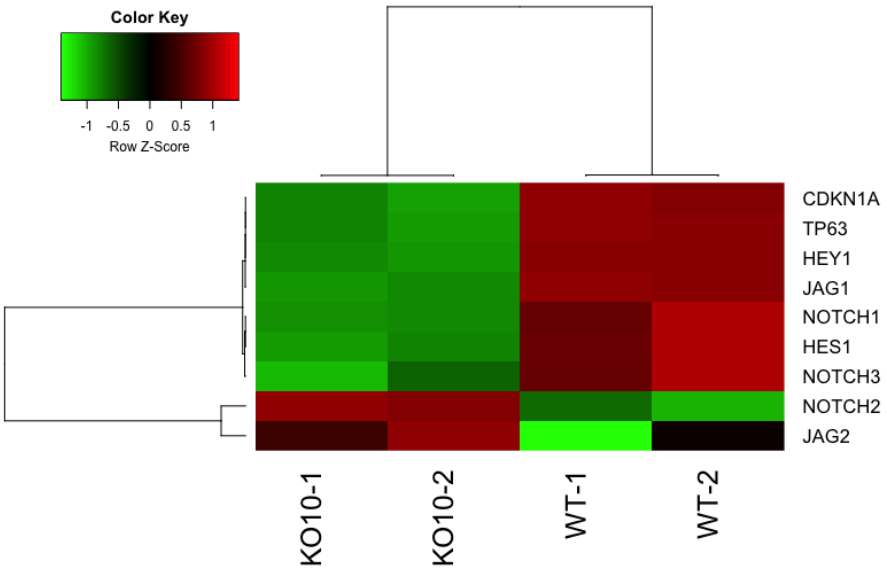

Figure S9. RNA sequencing of UM-UC-1 WT and FOXA1-KO cells. Heat map of RNA sequencing results for UM-UC-1 wild type and CRISPR edited UM-UC-1 FOXA1 knockout cells. The FOXA1 knockout cells had reduced expression of NOTCH1 compared to wild type.

References

1. Knowles, M. A. & Hurst, C. D. Molecular biology of bladder cancer: New insights into pathogenesis and clinical diversity. *Nat. Rev. Cancer* **15**, 25–41 (2015).
2. Kamat, A. M. *et al.* Bladder cancer. *Lancet (London, England)* **388**, 2796–2810 (2016).
3. Sanli, O. *et al.* Bladder cancer. *Nat. Rev. Dis. Prim.* **3**, 17022 (2017).
4. Shah, J. B., McConkey, D. J. & Dinney, C. P. N. New strategies in muscle-invasive bladder cancer: On the road to personalized medicine. *Clin. Cancer Res.* **17**, 2608–2612 (2011).
5. Warrick, J. I. *et al.* Intratumoral Heterogeneity of Bladder Cancer by Molecular Subtypes and Histologic Variants. *Eur. Urol.* 0–4 (2018). doi:10.1016/j.eururo.2018.09.003
6. Metts, M. C., Metts, J. C., Milito, S. J. & Thomas, C. R. Bladder cancer: a review of diagnosis and management. *J. Natl. Med. Assoc.* **92**, 285–294 (2000).
7. Chen, C. *et al.* Bladder Tumor Heterogeneity: The Impact on Clinical Treatment. *Urol. Int.* **95**, 1–8 (2015).
8. Cancer Genome Atlas Research Network, T. Comprehensive molecular characterization of urothelial bladder carcinoma. *Nature* **507**, 315–322 (2014).
9. Choi, W. *et al.* Identification of Distinct Basal and Luminal Subtypes of Muscle-Invasive Bladder Cancer with Different Sensitivities to Frontline Chemotherapy. *Cancer Cell* **25**, 152–165 (2014).
10. Damrauer, J. S. *et al.* Intrinsic subtypes of high-grade bladder cancer reflect the hallmarks of breast cancer biology. *Proc. Natl. Acad. Sci. U. S. A.* **111**, 3110–3115 (2014).
11. Hovelson, D. H. *et al.* Targeted DNA and RNA Sequencing of Paired Urothelial and Squamous Bladder Cancers Reveals Discordant Genomic and Transcriptomic Events and Unique Therapeutic Implications. *Eur. Urol.* **74**, 741–753 (2018).
12. Thomsen, M. B. H. *et al.* Comprehensive multiregional analysis of molecular heterogeneity in bladder cancer. *Sci. Rep.* **7**, 1–9 (2017).
13. Artavanis-Tsakonas, S., Rand, M. D. & Lake, R. J. Notch signaling: Cell fate control and signal integration in development. *Science (80-.).* **284**, 770–776 (1999).
14. Maraver, A. *et al.* NOTCH pathway inactivation promotes bladder cancer progression. *J. Clin. Invest.* **125**, 824–830 (2015).
15. Shutter, J. R. Dll4, a novel Notch ligand expressed in arterial endothelium. *Genes Dev.* **14**, 1313–1318 (2000).

16. Bray, S. J. Notch signalling in context. *Nat. Rev. Mol. Cell Biol.* **17**, 722–735 (2016).
17. Fernandez-marcos, P. J., Serrano, M. & Maraver, A. Bladder cancer and the Notch pathway. *Oncotarget* **6**, 1346–1347 (2015).
18. Goriki, A. *et al.* Unravelling disparate roles of NOTCH in bladder cancer. *Nat. Rev. Urol.* **15**, 345–357 (2018).
19. Benedito, R. *et al.* The Notch Ligands Dll4 and Jagged1 Have Opposing Effects on Angiogenesis. *Cell* **137**, 1124–1135 (2009).
20. Riahi, R. *et al.* Notch1-Dll4 signalling and mechanical force regulate leader cell formation during collective cell migration. *Nat. Commun.* **6**, 1–11 (2015).
21. Cohen, M., Georgiou, M., Stevenson, N. L., Miodownik, M. & Baum, B. Dynamic Filopodia Transmit Intermittent Delta-Notch Signaling to Drive Pattern Refinement during Lateral Inhibition. *Dev. Cell* **19**, 78–89 (2010).
22. Lee, S. H. *et al.* Tumor Evolution and Drug Response in Patient-Derived Organoid Models of Bladder Cancer. *Cell* **173**, 515-528.e17 (2018).
23. Mullenders, J. *et al.* Mouse and human urothelial cancer organoids: A tool for bladder cancer research. *Proc. Natl. Acad. Sci.* **116**, 4567–4574 (2019).
24. Ringuette Goulet, C. *et al.* Tissue-engineered human 3D model of bladder cancer for invasion study and drug discovery. *Biomaterials* **145**, 233–241 (2017).
25. Griffith, L. G. & Swartz, M. A. Capturing complex 3D tissue physiology in vitro. *Nat. Rev. Mol. Cell Biol.* **7**, 211–224 (2006).
26. Clark, A. G. & Vignjevic, D. M. Modes of cancer cell invasion and the role of the microenvironment. *Curr. Opin. Cell Biol.* **36**, 13–22 (2015).
27. Dean, Z. S., Elias, P., Jamilpour, N., Utzinger, U. & Wong, P. K. Probing 3D collective cancer invasion using double-stranded locked nucleic acid biosensors. *Anal. Chem.* **88**, 8902–8907 (2016).
28. Liu, L. *et al.* Minimization of thermodynamic costs in cancer cell invasion. *Proc. Natl. Acad. Sci. U. S. A.* **110**, 1686–1691 (2013).
29. Li, Y. H. & Zhu, C. A modified Boyden chamber assay for tumor cell transendothelial migration in vitro. *Clin. Exp. Metastasis* **17**, 423–429 (1999).
30. Bersini, S. *et al.* A microfluidic 3D invitro model for specificity of breast cancer metastasis to bone. *Biomaterials* **35**, 2454–2461 (2014).

31. Cheung, K. J. & Ewald, A. J. Invasive leader cells: Metastatic oncotarget. *Oncotarget* **5**, 1390–1391 (2014).
32. Droller, M. J. Biological considerations in the assessment of urothelial cancer: A retrospective. *Urology* **66**, 66–75 (2005).
33. Sara Bouhout, Alexandre Rousseau, Stéphane Chabaud, A. M. and S. B. Potential of Different Tissue Engineering Strategies in the Bladder Reconstruction. in *Regenerative Medicine and Tissue Engineering* doi:http://dx.doi.org/10.5772/55838
34. Habuchi, T. *et al.* Metachronous multifocal development of urothelial cancers by intraluminal seeding. *Lancet* **342**, 1087–1088 (1993).
35. Harris, A. L. & Neal, D. E. Bladder Cancer — Field versus Clonal Origin. *N. Engl. J. Med.* **326**, 759–761 (1992).
36. Sidransky, D. *et al.* Clonal Origin of Bladder Cancer. *N. Engl. J. Med.* **326**, 737–740 (1992).
37. Lunec, J., Challen, C., Wright, C., Mellon, K. & Neal, D. E. c-erbB-2 amplification and identical p53 mutations in concomitant transitional carcinomas of renal pelvis and urinary bladder. *Lancet* **339**, 439–440 (1992).
38. Glentis, A., Gurchenkov, V. & Vignjevic, D. M. Assembly, heterogeneity, and breaching of the basement membranes. *Cell Adh. Migr.* **8**, 236–245 (2014).
39. Lee, G. Y., Kenny, P. A., Lee, E. H. & Bissell, M. J. Three-dimensional culture models of normal and malignant breast epithelial cells. *Nat. Methods* **4**, 359–365 (2007).
40. Torab, P. *et al.* Three-Dimensional Microtumors for Probing Heterogeneity of Invasive Bladder Cancer. *Anal. Chem.* **92**, 8768–8775 (2020).
41. Roeder, B. A., Kokini, K., Sturgis, J. E., Robinson, J. P. & Voytik-Harbin, S. L. Tensile Mechanical Properties of Three-Dimensional Type I Collagen Extracellular Matrices With Varied Microstructure. *J. Biomech. Eng.* **124**, 214 (2002).
42. Sung, K. E. *et al.* Control of 3-dimensional collagen matrix polymerization for reproducible human mammary fibroblast cell culture in microfluidic devices. *Biomaterials* **30**, 4833–4841 (2009).
43. Doyle, A. D. Generation of 3D Collagen Gels with Controlled Diverse Architectures. *Curr. Protoc. Cell Biol.* **72**, 1–22 (2016).
44. Achilli, M. & Mantovani, D. Tailoring mechanical properties of collagen-based scaffolds for vascular tissue engineering: The effects of pH, temperature and ionic strength on

gelation. *Polymers (Basel).* **2**, 664–680 (2010).

45. Warrick, J. I. *et al.* FOXA1, GATA3 and PPARIγ Cooperate to drive luminal subtype in bladder cancer: A molecular analysis of established human cell lines. *Sci. Rep.* **6**, 1–15 (2016).
46. Zuiverloon, T. C. M., De Jong, F. C., Costello, J. C. & Theodorescu, D. Systematic Review: Characteristics and Preclinical Uses of Bladder Cancer Cell Lines. *Bl. Cancer* **4**, 169–183 (2018).
47. Luo, Y. *et al.* Characteristics of bladder transitional cell carcinoma with E-cadherin and N-cadherin double-negative expression. *Oncol. Lett.* **12**, 530–536 (2016).
48. Fujiyama, C. *et al.* Human bladder cancer invasion model using rat bladder in vitro and its use to test mechanisms and therapeutic inhibitors of invasion. *Br. J. Cancer* **84**, 558–564 (2001).
49. Jäger, W. *et al.* Minimally invasive establishment of murine orthotopic bladder xenografts. *J. Vis. Exp.* 1–10 (2014). doi:10.3791/51123
50. Wang, S., Sun, J., Zhang, D. D. & Wong, P. K. A nanobiosensor for dynamic single cell analysis during microvascular self-organization. *Nanoscale* **8**, 16894–16901 (2016).
51. Xiao, Y., Riahi, R., Torab, P., Zhang, D. D. & Wong, P. K. Collective Cell Migration in 3D Epithelial Wound Healing. *ACS Nano* **13**, 1204–1212 (2019).
52. Wang, S., Xiao, Y., Zhang, D. D. & Wong, P. K. A gapmer aptamer nanobiosensor for real-time monitoring of transcription and translation in single cells. *Biomaterials* **156**, 56–64 (2018).
53. Wang, S., Riahi, R., Li, N., Zhang, D. D. & Wong, P. K. Single Cell Nanobiosensors for Dynamic Gene Expression Profiling in Native Tissue Microenvironments. *Adv. Mater.* **27**, 6034–6038 (2015).
54. Riahi, R. *et al.* Mapping photothermally induced gene expression in living cells and tissues by nanorod-locked nucleic acid complexes. *ACS Nano* **8**, 3597–3605 (2014).
55. Dean, Z. S., Riahi, R. & Wong, P. K. Spatiotemporal dynamics of microRNA during epithelial collective cell migration. *Biomaterials* **37**, 156–163 (2015).
56. Hellström, M. *et al.* Dll4 signalling through Notch1 regulates formation of tip cells during angiogenesis. *Nature* **445**, 776–780 (2007).
57. Wang, S. *et al.* Intercellular Tension Negatively Regulates Angiogenic Sprouting of

Endothelial Tip Cells via Notch1-Dll4 Signaling. *Adv. Biosyst.* **1**, 1–23 (2017).

58. Fortini, M. E. Notch Signaling: The Core Pathway and Its Posttranslational Regulation. *Dev. Cell* **16**, 633–647 (2009).
59. Patel, N. S. *et al.* Up-regulation of endothelial delta-like 4 expression correlates with vessel maturation in bladder cancer. *Clin. Cancer Res.* **12**, 4836–4844 (2006).
60. Seifert, H. H. *et al.* A new and reliable culture system for superficial low-grade urothelial carcinoma of the bladder. *World J. Urol.* **25**, 297–302 (2007).
61. ATCC Primary Cell Culture Guide.
62. Jubb, A. M. *et al.* Expression of delta-like ligand 4 (Dll4) and markers of hypoxia in colon cancer. *Br. J. Cancer* **101**, 1749–1757 (2009).
63. Gurney, A. & Hoey, T. Anti-DLL4, a cancer therapeutic with multiple mechanisms of action. *Vasc. Cell* **3**, 2–5 (2011).
64. Kuhnert, F., Kirshner, J. R. & Thurston, G. Dll4-Notch signaling as a therapeutic target in tumor angiogenesis. *Vasc. Cell* **3**, 1–8 (2011).
65. Hoey, T. *et al.* DLL4 Blockade Inhibits Tumor Growth and Reduces Tumor-Initiating Cell Frequency. *Cell Stem Cell* **5**, 168–177 (2009).
66. Warrick, J. I. *et al.* FOXA1 and CK14 as markers of luminal and basal subtypes in histologic variants of bladder cancer and their associated conventional urothelial carcinoma. *Virchows Arch.* **471**, 337–345 (2017).
67. DeGraff, D. J. *et al.* When urothelial differentiation pathways go wrong: Implications for bladder cancer development and progression. *Urol. Oncol. Semin. Orig. Investig.* **31**, 802–811 (2013).

Vita

Education

Doctor of Philosophy in Mechanical Engineering — *August 2015 – December 2020*
The Pennsylvania State University, University Park, PA

Master of Science in Mechanical Engineering — *August 2013 – May 2015*
Gannon University, Erie, PA

Bachelor of Science in Mechanical Engineering — *August 2008 – May 2013*
Rochester Institute of Technology, Rochester, NY

Publications

Peter Torab, Britney Forsyth, Tyler Malcolm, Yi Lu, Pak Kin Wong, "A Rapid Bacterial Enrichment Technique for Sepsis Detection and Antimicrobial Susceptibility Testing", To be submitted

Brian Scherer, Christine Surrette, Hui Li, **Peter Torab**, Erik Kvam, Craig Galligan, Steven Go, Greg Grossmann, Tyler Hammond, Tammy Johnson, Richard St-Pierre, John Nelson, Radislav Potyrailo, Tejas Khire, Kuangwen Hsieh, Jeff Want, Pak Kin Wong, Chris Puleo, "Digital Electrical Impedance Analysis for Single Bacterium Sensing and Antimicrobial Susceptibility Testing", Under review

Peter Torab, Yue Yan, Hironobu Yamashita Joshua I. Warrick, Jay D. Raman, David J. DeGraff, Pak Kin Wong, "Three-Dimensional Microtumors Reveal Heterogeneity of Invasive Bladder Cancer", *ACS Analytical Chemistry,* June 2020

Hui Li, **Peter Torab**, Pak Kin Wong, "Detection of bacterial infection via a fidget spinner", *Nature Biomedical Engineering,* June 2020

Hui Li, **Peter Torab**, Kathleen E. Mach, Christine Surrette, Matthew R. England, David W. Craft, Neal J. Thomas, Joseph C. Liao, Chris Puleo, Pak Kin Wong, "Adaptable microfluidic system for single-cell pathogen classification and antimicrobial susceptibility testing", *Proceedings of the National Academy of Sciences,* May 2019

Yuan Xiao, Reza Riahi, **Peter Torab**, Donna D. Zhang, Pak Kin Wong, "Collective Cell Migration in 3D Epithelial Wound Healing", *ACS Nano,* 2019

Jian Gao, Hui Li, **Peter Torab**, Kathleen E. Mach, David W. Craft, Neal J. Thomas, Chris M. Puleo, Joseph C. Liao, Tza-Huei Wang, Pak Kin Wong, "Nanotube assisted microwave electroporation for single cell pathogen identification and antimicrobial susceptibility testing", *Nanomedicine: Nanotechnology, Biology and Medicine*, Volume 17, 2019

Peter Torab, Davide Piovesan, "Vibrations of fractal structures: on the nonlinearities of damping by branching", *Journal of Nanotechnology in Engineering and Medicine,* 2015